Chapter 3 Mechanistic Investigation of Nitroxide-based Polymerization Inhibitors

3.1. Introduction

3.1.1. Nitroxide radicals

In the mechanistic studies of nitroxide-based polymerization inhibitors, nitroxide radicals act as monomer stabilizers and also as an important reporting agent. Nitroxide, also known as amine-*N*-oxide, is a functional group which contains an N-O bond and side groups attaching to the nitrogen (*e.g.* $R_3N{\rightarrow}O$). Nitroxide radicals, also known as nitroxyl radicals, have substantial life time which enables them to be widely used as persistent free radicals. In this thesis, the term of nitroxide refers to nitroxide radicals. The chemical structures are shown in Figure 3.1.

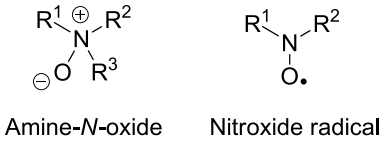

Figure 3. 1. Chemical structure of amine-*N*-oxide and nitroxide radicals.

A nitroxide radical is generally an oxygen-centred radical with the free electron delocalised over the N-O bond. Spin density on the oxygen atom can be clearly observed from the EPR spectrum of ^{17}O-labelled TEMPO.[1] The resonance structures for nitroxide radicals are shown in Scheme 3.1. The resonance effect contributes to the stability of such radicals.

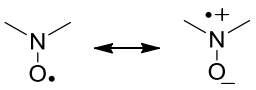

Scheme 3. 1. Resonance structures of nitroxide radicals.

3.1.1.1. Synthesis of nitroxide radicals

Amine-*N*-oxides are normally synthesized by oxidation of amines or pyridine analogs with hydrogen peroxide or peracids (Scheme 3.2).

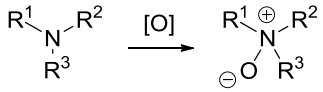

Scheme 3. 2. Oxidation of an amine to an amine-*N*-oxide.

If a secondary amine is oxidized by hydrogen peroxide or peracids, very often a nitroxide radical is formed. Oxidation of secondary amines lacking α-hydrogens leads to particularly persistent nitroxide radicals[2] (Scheme 3.3). The steric effect also contributes to the stability of the radicals.

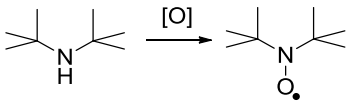

Scheme 3. 3. Oxidation of a sterically protected secondary amine to a nitroxide radical.

Organic radicals are often highly reactive and unstable. However, sterically protected and resonance stabilized organic radicals have been prepared and explored. A series of nitroxide radicals with appreciable life time has been synthesized in the last 50 years[3]. Some common nitroxide radicals are shown in Figure 3.2.

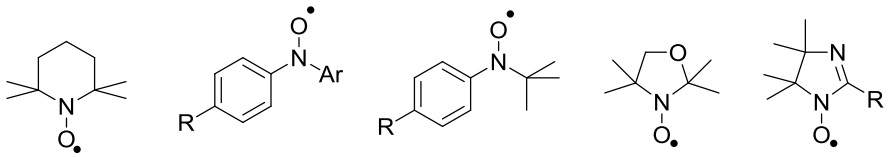

Figure 3. 2. Common persistent nitroxide radicals.

Among these structures, TEMPO (2,2,6,6-tetramethylpiperidine-1-oxyl) derivatives (Figure 3.3) are the most widely used nitroxide radicals due to their remarkable persistency. TEMPO is a red-orange solid at ambient conditions. It was discovered

by Lebedev and Kazarnowskii[4] in 1960. TEMPO is usually prepared by oxidation of 2,2,6,6-tetramethylpiperidine with hydrogen peroxide.

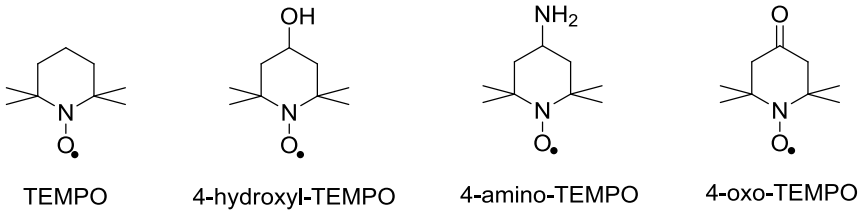

Figure 3. 3. Structures of common TEMPO derivatives.

3.1.1.2. General chemistry of nitroxide radicals

Oxidation and reduction

The redox reactions of nitroxide radicals have attracted much attention in the past few decades. One electron oxidation of nitroxide radicals gives the corresponding *N*-oxoammonium cation, and one electron reduction leads to the aminoxyl anion (Scheme 3.4).

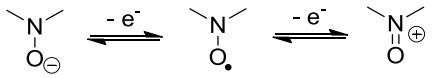

Scheme 3. 4. Redox reactions of nitroxide radical.

Similarly, the redox couples of TEMPO derivatives are well-known. Interconversion of different oxidative states of TEMPO (Scheme 3.5) is in fact the basis for many applications. The oxidation and reduction potential of TEMPO are 0.76V and 1.48V[5], respectively.

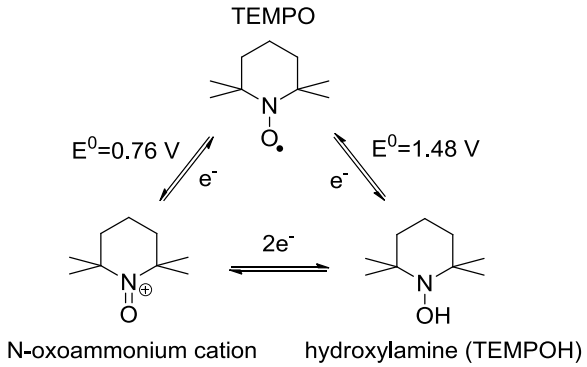

Scheme 3. 5. Interconversion of TEMPO, hydroxylamine and *N*-oxoammonium cation.

The product of one electron oxidation of TEMPO, the corresponding *N*-oxoammonium cation, is a strong oxidizing agent. *N*-oxoammonium cation is often prepared by oxidation of TEMPO with halogens. The counter anion of the oxoammonium cation is therefore usually chloride or bromide. Such salts can be isolated. Golubev *et al.* discovered *N*-oxoammonium salt[6-7], and pioneered the studies of its application as an oxidizing agent[8].

TEMPO hydroxylamine (TEMPOH) is formed by one electron reduction of TEMPO. It is usually synthesized by reduction of TEMPO under mild conditions (*e.g.* ascorbate). In air, TEMPOH can be readily oxidized back to TEMPO. The applications of TEMPO in biochemistry often relate to its reduction to TEMPOH. In such systems, reduction of TEMPO usually involves metal ions[9] (Scheme 3.6).

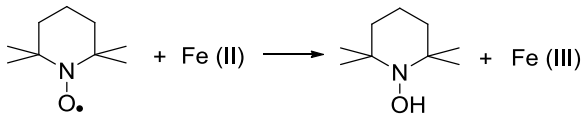

Scheme 3. 6. Reduction of TEMPO by ferrous iron.

Disproportionation reaction

Sterically protected nitroxide radicals have appreciable life time, however, if one or more α-hydrogens present, nitroxide radicals can decompose to the corresponding hydroxylamine and a nitrone[10] (Scheme 3.7).

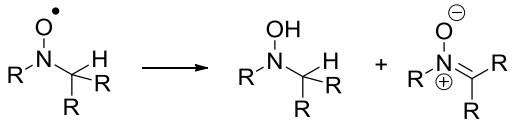

Scheme 3. 7. Decomposition of nitroxide radicals with one or more α-hydrogen atoms.

TEMPO is stabilized by the α-methyl groups, and hence does not undergo such reactions spontaneously. Instead, acid catalyzed disproportionation is a featured reaction of TEMPO derivatives. Protonation of TEMPO is followed by a disproportionation reaction which leads to formation of TEMPOH and *N*-oxoammonium cation[11] (Scheme 3.8).

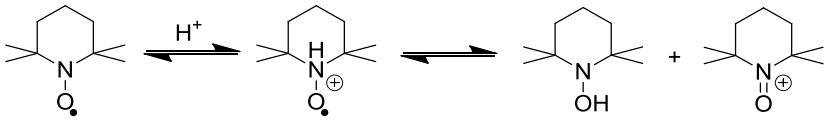

Scheme 3. 8. Protonation and disproportionation reaction of TEMPO.

Hydrogen abstraction by nitroxide radicals and antioxidant reactions of hydroxylamines

This section considers the thermodynamic and kinetic aspects of hydrogen abstraction reaction of nitroxide radicals and hydroxylamines. As persistent radicals, TEMPO derivatives are inert compared to many other organic radicals (*e.g.* alkyl). The persistency leads to many of their applications in EPR spectroscopy. In biochemistry, their applications are often related to the hydrogen abstraction reactions. Generally, nitroxide radicals can abstract hydrogen atoms from molecules with labile hydrogen and form the corresponding hydroxylamine (Scheme 3.9). This reaction is often reversible. The reverse reaction, hydrogen abstraction from hydroxylamines is the basis of their antioxidant properties.

Scheme 3. 9. Hydrogen abstraction by nitroxide radical.

Similarly, hydrogen abstraction is also essential to the antioxidant properties of many phenols[12] (*e.g.* 4-methoxyphenol). Some common phenols and hydroxylamines are shown in Figure 3.4.

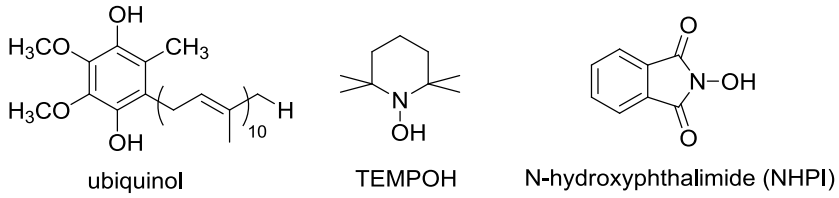

Figure 3. 4. Chemical structures of ubiquinol, TEMPOH and N-hydroxylphthalimide (NHPI).

Bond Dissociation Enthalpies (BDEs) of the O-H bond in the corresponding compounds can be used to qualitatively predict their hydrogen abstraction abilities. BDEs of hydroxylamines can be compared to phenols (Table 3.1).

Table 3. 1. Bond dissociation enthalpies of O-H bonds in some R_2NOH compounds and phenols.

Molecule	BDE(O-H)/kJ·mol^{-1}
TEMPOH[13]	299.2
N-hydroxyphthalimide (NHPI)[14]	364
phenol[15]	362
4-MeO-phenol[15]	340.2
2,4,6-$(MeO)_3$-phenol[15]	303.8
ubiquinol ($CoQH_2$)[15]	310.5

Generally, higher BDE suggests lower reactivity of the O-H bond thus higher reactivity of the corresponding nitroxide or phenoxyl radical. As shown in Table 3.1, TEMPOH has a lower BDE(O-H) than other R_2NOH compounds (*e.g.* NHPI). This effect is due to the steric hindrance. Therefore, hydrogen abstraction by TEMPO (Scheme 3.10) is more difficult compared to some other types of nitroxide radicals.

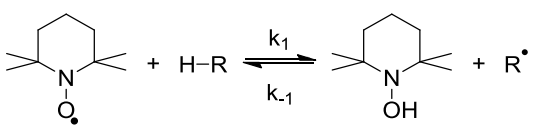

Scheme 3. 10. Reversible hydrogen abstraction to TEMPO.

Evidently, thermodynamics of the reaction shown in Scheme 3.10 also depends on the BDE(R-H) of the substrate (Table 3.2).

Table 3. 2. Bond dissociation enthalpies of R-H bonds.

Molecule	BDE(R-H)/kJ·mol^{-1}
C_2H_5-**H**	423
$C_6H_5CH_2$-**H**	376
CH_2=CH-**H**[16]	460
HO-**H**	497
CH_3O-**H**	436
CH_3OO-**H**[17]	360
*n*BuOO-**H**[17]	358

Since BDE(R-H) in these compounds are generally higher than BDE(O-H) in hydroxylamines and phenols, the reverse reaction is favourable. Kinetically, the reaction rate k_1 of hydrogen abstraction from hydrocarbons (RH) by TEMPO is *ca.* 10^{-6} to 10^{-4} $M^{-1}\cdot s^{-1}$, which is significantly slower than the reverse reaction (k_{-1}=10 to 10^4 $M^{-1}\cdot s^{-1}$)[18]. The reverse reaction, hydrogen abstraction from hydroxylamines and phenols, is the basis for antioxidant applications of these compounds. In a general antioxidant process, reactive radicals are quenched, while the antioxidant loses a hydrogen atom and forms a less reactive radical (Scheme 3.11).

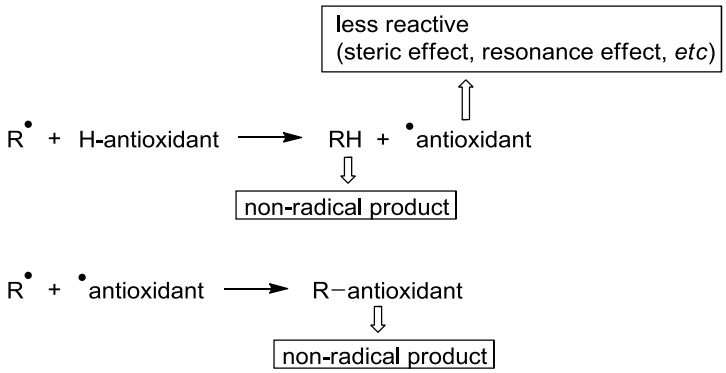

Scheme 3. 11. General antioxidant reaction via hydrogen abstraction.

Since the change in entropy (ΔS) of hydrogen abstraction reaction is often negligible, if solvent effect is disregarded, Gibbs function (ΔG) relies on the enthalpies of O-H bond breaking and R-H bond formation. Comparing the BDE values, hydrogen

abstraction by hydroxyl and alkyl radicals is thermodynamically favourable. Peroxyl radicals (ROO$^{\bullet}$), due to lower BDE(ROO-H) of the corresponding peroxides, are less reactive. Antioxidants with lower BDE(O-H) are required in order to quench peroxyl radicals. Thus, a good antioxidant is usually characterized by a low BDE(O-H) value (*e.g.* ubiquinol, TEMPOH).

Hydrogen abstraction can be described as a one-step hydrogen atom transfer (HAT) reaction. Alternatively, it can also be illustrated in two-step pathways in which hydrogen abstraction can be explained by an electron transfer (oxidation/reduction) and a protonation process (Scheme 3.12).[19]

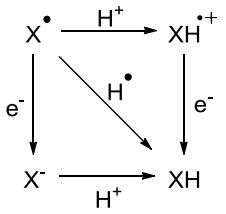

Scheme 3. 12. Reaction pathways from X$^{\bullet}$ to XH.

By using this thermodynamic cycle, BDE of TEMPOH can be related to redox potentials and pK_a values of the corresponding species (Scheme 3.13).

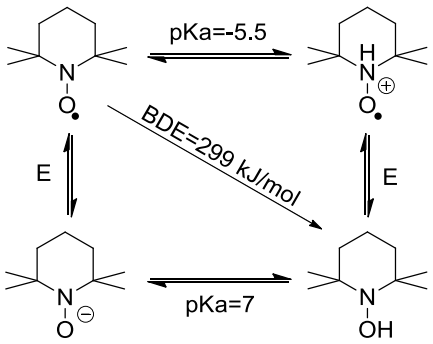

Scheme 3. 13. Reaction pathways of TEMPO to TEMPOH.

The semiempirical relation between BDE, pKa and redox potential can be described by Equation 3.1[20].

$$BDE_{XH} = 1.37\,pKa - 23.1E_{ox}(X^{-}) + 73.3kcal \cdot mol^{-1} \qquad (3.1)$$

Here, BDE_{XH} is bond dissociation enthalpy of X-H in kcal·mol^{-1}, $E_{ox}(X^-)$ is the oxidation potential of the conjugated base X^- in eV.

Radical reactions of TEMPO, TEMPOH and N-oxoammonium cation

TEMPO is inert compared to alkyl radicals due to steric hindrance and resonance effect. Dimerization of TEMPO is very slow. However, highly reactive radicals (*e.g.* alkyl) can react with TEMPO via an addition reaction (Scheme 3.14).

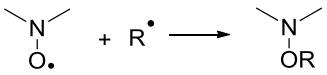

Scheme 3. 14. Quenching of a reactive radical R$^{\bullet}$ by a nitroxide radical via addition.

Reactions between TEMPO and alkyl radicals are fast. The reaction rate of TEMPO with primary alkyl radicals[21] is *ca.* 10^9 $M^{-1}\cdot s^{-1}$ at 60 ℃. These reactions are sometimes reversible[22] because O-R bond in the product, alkoxyamine, is relatively easy to break. Table 3.3 shows the bond dissociation enthalpies[23] of the NO-R bond in some alkoxyamines. Compared to BDE(O-H) in hydroxylamines and phenols (Table 3.1, p82), these products are less stable. The reversible reaction between TEMPO and alkyl radicals is particularly important in living radical polymerization. The application of TEMPO in mediating living radical polymerization will be discussed in Section 3.1.1.3 (p88).

Table 3. 3. Bond dissociation enthalpies of some alkoxyamines.

Alkoxyamine	BDE(NO-R)/kJ·mol^{-1}
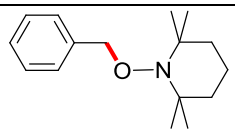	128.9
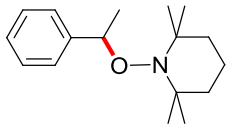	118.8
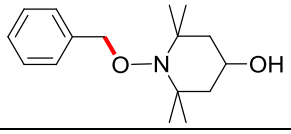	131.4

Apart from radical addition, nitroxides can undergo redox reactions with other radicals. Many applications of TEMPO redox couples in biochemistry are related to quenching reactive radicals. Inter-conversion of TEMPO, TEMPOH and *N*-oxoammonium cation, and their reactions with superoxide and hydroperoxyl radicals[9, 24] are particularly important (Scheme 3.15).

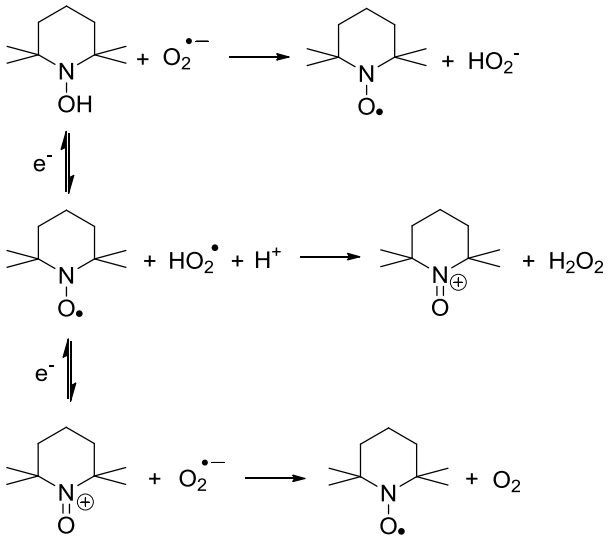

Scheme 3. 15. Inter-conversion of TEMPO, TEMPOH and *N*-oxoammonium cation and their reactions with superoxide/hydroperoxyl radicals.

3.1.1.3. Applications of TEMPO derivatives

Applications of TEMPO mainly include mediating free radical polymerization[25-27], as polymerization inhibitors[28], applications in Electron Paramagnetic Resonance (EPR) spectroscopy[29], antioxidant[30-32] in biochemistry and catalysts in organic synthesis[33-37]. Some of the applications are associated with the fact that TEMPO derivatives are persistent free radicals. Some other applications are due to their redox chemistry.

Applications in organic synthesis

TEMPO catalyzed alcohol oxidation is widely used in organic synthesis. In many cases, a second oxidizing agent is required to oxidize TEMPO to *N*-oxoammonium

cation which is the primary oxidant. An example catalytic cycle[36] is shown in scheme 3.16.

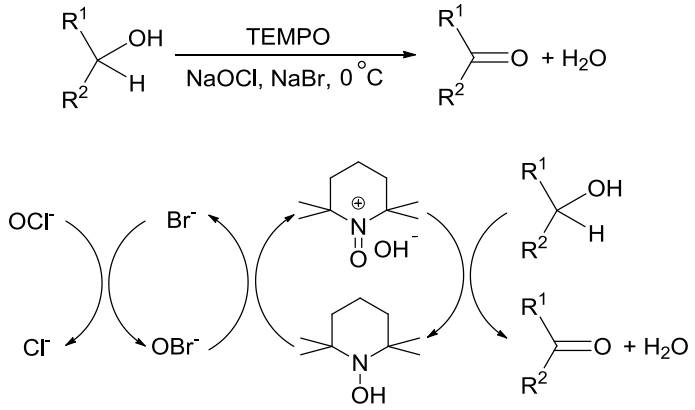

Scheme 3. 16. TEMPO catalyzed oxidation reaction of alcohols.

In this reaction, bleach (NaOCl) acts as the secondary oxidizing agent required to synthesize the *N*-oxoammonium cation *in situ* via oxidation of TEMPO. The oxoammonium salt, which is generated *in situ* by oxidation of a catalytic amount of nitroxide with a stoichiometric amount of a secondary oxidant, has thus been extensively used in the oxidation of primary and secondary alcohols. These oxidation reactions lead to the corresponding aldehydes, ketones[33] and sometimes carboxylic acids and ethers[38-39]. This type of reactions drew much attention due to its metal-free, environmentally friendly and highly selective nature, which brings significant advantages, particularly in pharmaceutical industry.

Applications in biochemistry

Interconversion between TEMPO, TEMPOH and *N*-oxoammonium cation and their abilities to scavenge reactive radicals in biological systems is often exploited in their applications in biochemistry. As effective antioxidants, TEMPO derivatives and their redox couples can act as protective agents in a range of biological models of oxidative stress and ageing. For instance, inflammation often leads to an increase in the formation of reactive oxygen species including superoxide and hydroperoxyl radicals. Functionalized hydroxylamine was studied as a potential diagnostic tool for inflammation-induced oxidative stress[32], as the formation of the corresponding

TEMPO derivative can be monitored by EPR spectroscopy. The result shows that the detection limit of superoxide radicals formation by functionalized hydroxylamine is 10 times lower than for the other spin traps such as DEPMPO (5-(diethoxyphosphoryl)-5-methyl-1-pyrroline-*N*-oxide). The chemical reaction is shown in Scheme 3.17.

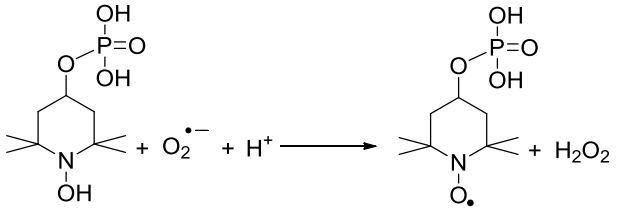

Scheme 3. 17. Reaction of functionalized hydroxylamine with superoxide radical.

Mediating living radical polymerization

Free radical polymerization typically results in polydisperse polymers due to various termination mechanisms. Living radical polymerization relies on termination-free propagation so that monodisperse polymers and block copolymers can be made. TEMPO derivatives are common mediators of living radical polymerization, particularly for styrene. As shown in Scheme 3.14 (p85), TEMPO can react with alkyl radicals. This reversible reaction can be used to control radical polymerization. TEMPO and the propagation radical can achieve a dynamic equilibrium with the addition product alkoxyamine (Scheme 3.18). Under thermal conditions, homolytic dissociation of the alkoxyamine can regenerate TEMPO and the reactive carbon-centred radical, thus can restart the chain propagation. Here, TEMPO acts as a controlling agent. The concentration of TEMPO can be used to shift the equilibrium, thus control the rate of polymerization.

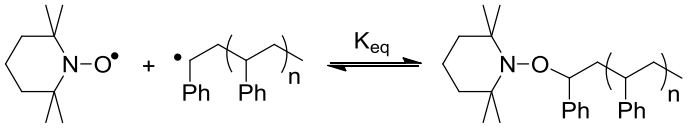

Scheme 3. 18. TEMPO initiated and mediated living radical polymerization of styrene.

Applications as polymerization inhibitor

Due to formation of dangerous chemicals (*e.g.* polyperoxides) in chain reactions and possible run-away polymerization, stabilizers are commonly used to inhibit polymerization during monomer storage. TEMPO derivatives are popular polymerization inhibitors. Particularly, 4-hydroxy-TEMPO (4HT) is widely used in industry to inhibit polymerization of a range of monomers. The investigation by Reichert *et al.* shows immediate termination of methyl methacrylate polymerization following addition of 4HT.[28] The induction period before polymerization resumes is proportional to 4HT concentration (Figure 3.5).

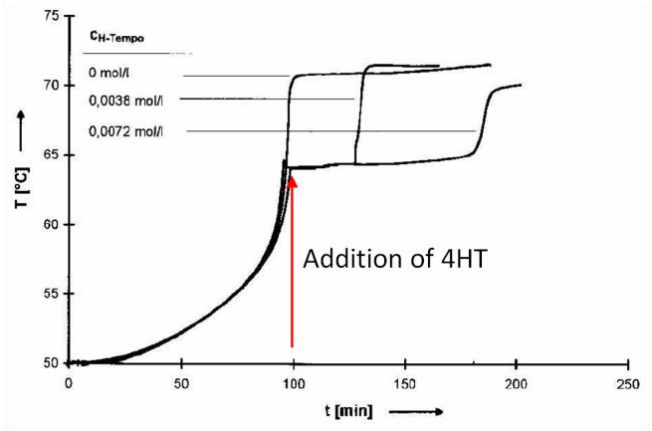

Figure 3. 5. Induction period induced by addition of 4HT to thermal polymerization of methyl methacrylate.

Due to the applications of TEMPO derivatives in polymerization systems, next section discusses the mechanism of free radical polymerization in detail.

3.1.2. Free radical polymerization and inhibition

Radical polymerization is an important type of polymerization in which chain propagation is a radical reaction. Compared to anionic and cationic polymerization, free radical polymerization is a relatively non-specific process which involves various termination and chain transfer mechanisms.

3.1.2.1. Initiation, propagation and termination steps

The initiation, propagation and termination steps of radical polymerization are shown in Scheme 3.19.

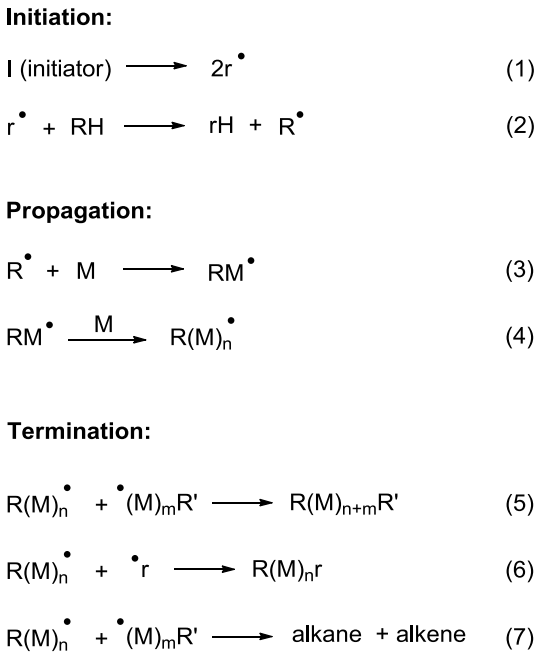

Scheme 3. 19. Common initiation, propagation and termination mechanisms of radical polymerization.

In the presence of initiator molecules, radicals ($r^{\bullet}$) are generated (reaction 1). These radicals can add to unsaturated bonds or undergo hydrogen abstraction from the substrate to form carbon-centred radicals $R^{\bullet}$ (reaction 2). The alkyl radicals further react with monomers (M) to start chain propagation (reaction 3 and 4). Reaction between alkyl radicals and monomers is fast. The reaction rate[21] at room temperature is *ca.* 10^5 $M^{-1}{\cdot}s^{-1}$ (Table 3.4).

Table 3. 4. Reaction rate between alkyl radicals ($R^{\bullet}$) and monomers at 25 ℃.

$R^{\bullet}$ \ monomer	styrene	methyl methacrylate
$CH_3^{\bullet}$	2.6×10^5 $M^{-1}{\cdot}s^{-1}$	4.9×10^5 $M^{-1}{\cdot}s^{-1}$
$(CH_3)_3C^{\bullet}$	1.3×10^5 $M^{-1}{\cdot}s^{-1}$	6.6×10^5 $M^{-1}{\cdot}s^{-1}$

The end chain can be terminated via radical combination (reaction 5 and 6) or dismutation with another propagation radical to form an alkane and an alkene (reaction 7).

There are various types of polymerization initiators, which provide different initiation radicals. Oxygen and carbon centred radicals are often generated to start chain reactions since they are more reactive. Organic peroxides and azo compounds are thus common initiators of radical polymerization (Scheme 3.20).

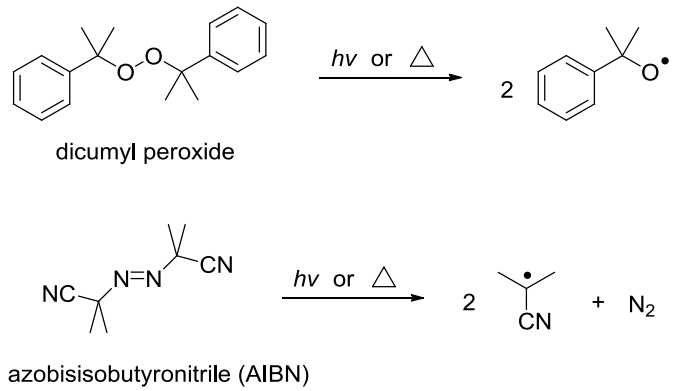

Scheme 3. 20. Free radical generation by dicumyl peroxide and AIBN.

The reaction between alkoxyl radicals and monomers is also efficient, but slightly slower than the reaction between alkyl radicals and monomers in general. The reaction rate[21] is *ca.* 10^5 $M^{-1}{\cdot}s^{-1}$ at 60 ℃ (Table 3.5).

Table 3. 5. Reaction rate between alkoxyl radical $(CH_3)_3CO^{\bullet}$ and monomers at 60 ℃.

RO• \ monomer	styrene	methyl methacrylate
$(CH_3)_3CO^{\bullet}$	9×10^5 $M^{-1}{\cdot}s^{-1}$	2.5×10^5 $M^{-1}{\cdot}s^{-1}$

3.1.2.2. Self-initiation mechanism

Spontaneous polymerization of organic monomers is the polymerization reaction in the absence of additional initiators. As shown in Scheme 3.21, if the monomer is exposed to heat or light, it can form carbon radicals directly (reaction 8). Then the carbon radical reacts with the other monomers to form polymer chains.

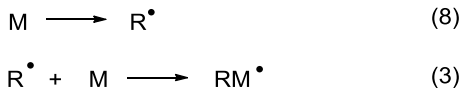

Scheme 3. 21. Formation of alkyl propagation chain in the absence of polymerization initiators

Self-initiation of spontaneous polymerization often involves complex reaction mechanisms. For instance, Mayo[40-41] mechanism was proposed to explain autoxidation of styrene (Scheme 3.22). Styrene molecules undergo Diels-Alder reaction which forms a dimer with a labile hydrogen atom. Another molecule of styrene can react with the dimer via molecule-assisted homolysis (MAH) mechanism and yields carbon-centred radicals which lead to initiation. The driving force of MAH mechanism is formation of an aromatic radical.

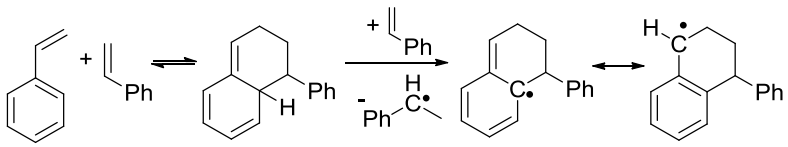

Scheme 3. 22. Self-initiation mechanism of styrene proposed by Mayo.[40-41]

In monomers lacking conjugated double bonds, Diels-Alder reaction is not possible. Thermal initiation, however, is a widely acknowledged mechanism for many monomers and monomer combinations. Initiation involves a biradical intermediate followed by hydrogen abstraction from H-donors[42-43] (Scheme 3.23).

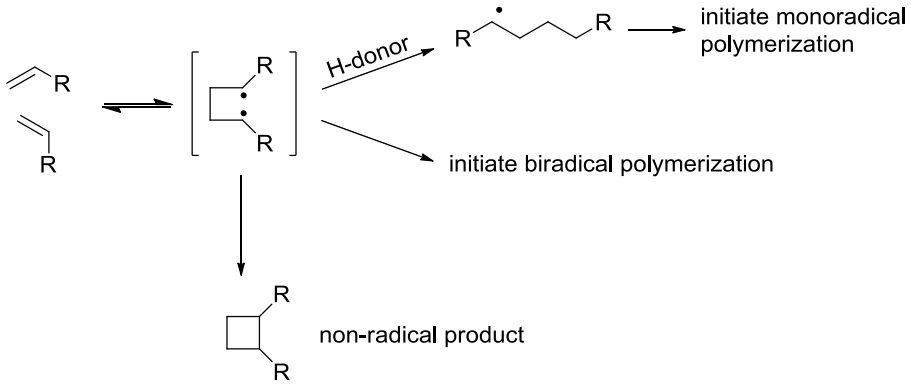

Scheme 3. 23. Thermal initiation mechanism.

It is not clear if thermal initiation is only related to monomer molecules, because trace amount of impurities could also initiate the mechanism. For instance, as shown in Scheme 3.24, peroxides can yield alkoxyl radicals $RO^{\bullet}$ by cleavage of the oxygen-oxygen single bond (reaction 9). The alkoxyl radicals can add to double bonds of the monomer molecule that leads to formation of propagation radicals (reaction 10).

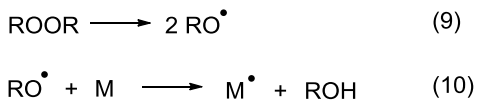

Scheme 3. 24. Organic peroxide initiation mechanism.

Metal salts can lead to redox initiation by reacting with the monomer (Scheme 3.25).

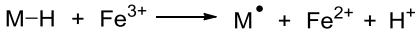

Scheme 3. 25. Initiation mechanism of iron(III).

Oxygen species can also initiate polymerization either by hydrogen abstraction or via addition reactions. Molecular oxygen can abstract hydrogen atoms from monomers and form alkyl radicals[44] (Scheme 3.26).

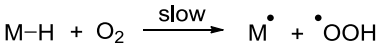

Scheme 3. 26. Hydrogen abstraction from monomer (M-H) by molecular oxygen.

Denisov[45] suggested that initiation by molecular oxygen is a termolecular process (Scheme 3.27), since this mehanism involves appreciably less energy than the bimolecular process. Hydrogen abstraction mechanism is particularly important for compounds containing weak R-H bonds. The reaction rate has been determined to be 1.2×10^{-9} $M^{-1} \cdot s^{-1}$ (at 127 ℃) in cyclohexane.[46]

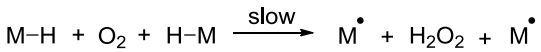

Scheme 3. 27. Termolecular initiation by O_2.

Compared to molecular oxygen, hydrogen abstraction by some reactive oxygen species is faster. For instance, O_2 could undergo one-electron reduction to superoxide ion $O_2^{\bullet-}$. Hydrogen abstraction from monomer by superoxide leads to formation of an initiation radical (Scheme 3.28).

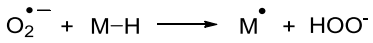

Scheme 3. 28. Hydrogen abstraction from monomer (M) to superoxide ion.

3.1.2.3. Inhibition and retardation mechanism

During monomer production and storage, spontaneous polymerization can be initiated via various mechanisms. To prevent the formation of dangerous chemicals (*e.g.* poly-peroxide) during monomer storage, inhibitors are used to scavenge the initiating species and the propagation radicals. There are mainly two reaction mechanisms by which inhibitors (IH) terminate the propagation radicals (Scheme 3.29). Reaction 11 illustrates a hydrogen abstraction mechanism. The propagation radical is terminated by abstracting a hydrogen atom from the inhibitor molecule, and forms a less reactive inhibitor radical $I^{\bullet}$. The second mechanism (reaction 12) is to quench the propagation radical via an addition reaction to form a relatively stable species $RIH^{\bullet}$. The radicals formed in these mechanisms (i.e. $I^{\bullet}$ and $RIH^{\bullet}$) are not reactive thus can neither add to double bonds nor abstract hydrogen atoms. Consequently they usually form non-radical products by combining with another radical or dismutation.

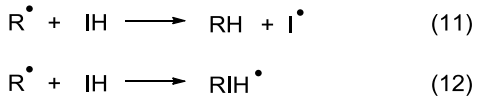

Scheme 3. 29. Hydrogen abstraction (reaction 11) and addition mechanism (reaction 12) of polymerization inhibition.

Different types of inhibitors follow different inhibition mechanisms. Hydrogen abstraction is typical for phenol- and amine-type inhibitors, while addition mechanism is common to nitroxide and quinone inhibitors. Some commercial

polymerization inhibitors are shown in Figure 3.6. The mechanism of different inhibitors is discussed in the following sections.

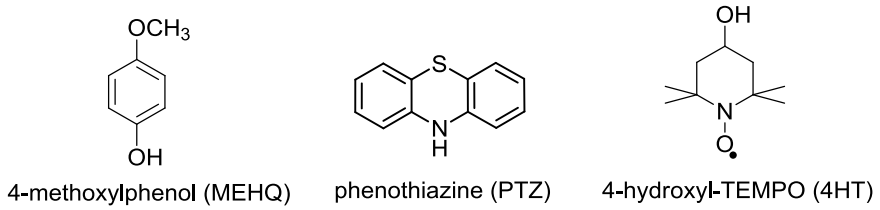

Figure 3. 6. Common polymerization inhibitors.

Dioxygen (O_2)

A number of polymerization inhibitors quench chain carrying radicals via addition reaction to form a less reactive species[46]. Molecular oxygen can be considered an inhibitor of this type, because of its reaction with the propagation radicals. As shown in Scheme 3.30, O_2 reacts with alkyl radicals ($R^{\bullet}$) rapidly (*ca.* 10^9 $M^{-1}{\cdot}s^{-1}$ at room temperature)[47] to form peroxyl radicals ($RO_2^{\bullet}$). When dissolved oxygen concentration is high, the formation of peroxyl radicals is significant because addition of propagation radicals to oxygen (reaction 13) is much faster than addition to monomers (Scheme 3.19, reaction 3, p90). For oxygen concentration above 10^{-4} M, the concentration of $RO_2^{\bullet}$ is much higher than $R^{\bullet}$.[47] Peroxyl radicals are much less reactive as compared to alkyl radicals. Reaction rate of peroxyl radical with styrene is 68 $M^{-1}{\cdot}s^{-1}$ at 25 ℃[46]. Hence, peroxyl radicals are not efficient in initiating chain propagation. Most peroxyl radicals terminate via reaction 14.

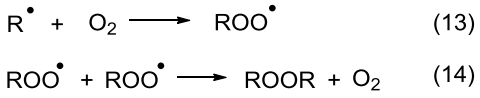

Scheme 3. 30. Formation and termination of propagation radical by peroxyl radicals.

Due to the mechanism shown in Scheme 3.30, molecular oxygen inhibits free radical polymerization. During this process, oxygen is consumed via its reaction with propagation radicals. Since this is a rapid reaction, as oxygen depletes, termination of peroxyl radicals leads to formation of organic peroxides (reaction 14). Thereafter, as shown in Scheme 3.24 (p93), homolytic cleavage of O-O bond releases more

reactive radicals and eventually promotes polymerization. Hence, extra polymerization inhibitors are commonly added to further stabilize monomers.

MEHQ

Many polymerization inhibitors (*e.g.* phenols) work best in the presence of oxygen because they intercept peroxyl radicals and decelerate oxygen consumption while stopping chain propagation. 4-Methoxyphenol (also known as monomethyl ether of hydroquinone, MEHQ) is an inhibitor of this type. The inhibition mechanism[48-50] is shown in Scheme 3.31.

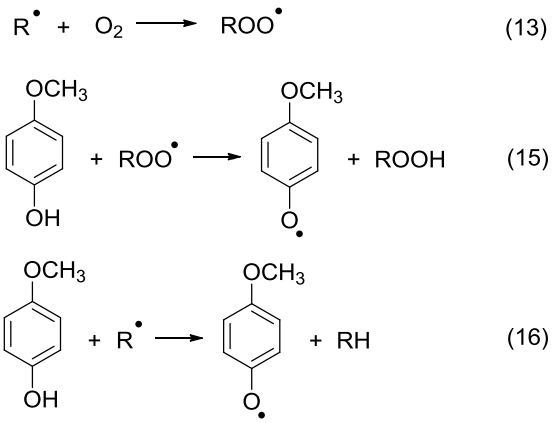

Scheme 3. 31. Inhibition mechanism of 4-methoxylphenol.

MEHQ quenches peroxyl radicals (reaction 15) and alkyl radicals (reaction 16) via the same hydrogen abstraction mechanism which leads to formation of a phenoxyl radical. The phenoxyl radical is less reactive because it is stabilized by resonance effect (Scheme 3.32).

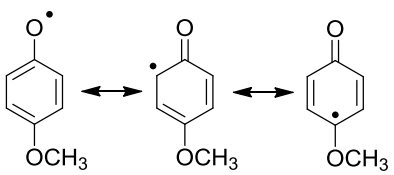

Scheme 3. 32. Resonance contributors of MEHQ phenoxyl radical.

However, direct quenching of alkyl radicals by MEHQ is not efficient. In fact, many phenols including MEHQ alone are poor polymerization inhibitors. During monomer storage, MEHQ alone cannot effectively inhibit polymerization in the absence of dissolved oxygen.

PTZ

Phenothiazine (PTZ) is a widely used polymerization inhibitor, particularly in acidic monomers (*e.g.* acrylic acid). The inhibition mechanism is completely different to MEHQ. MEHQ intercepts peroxyl radicals much more efficiently than quenching alkyl radicals, therefore efficacy of MEHQ largely depends on dissolved oxygen. PTZ can also react with peroxyl radicals via an electron transfer reaction to form a radical cation (Scheme 3.33). The radical cation of PTZ is stable, and its EPR spectrum is well-known. [51-52]

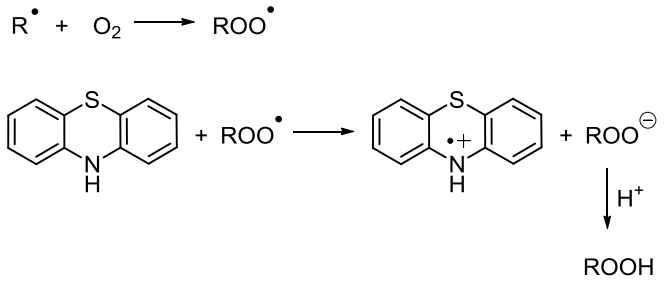

Scheme 3. 33. Reaction mechanism of PTZ with alkyl radicals in the presence of oxygen.

However, this is not the dominant mechanism since inhibition by PTZ does not depend on oxygen concentration. It was reported[53] that addition of alkyl radical to PTZ radical cation is responsible for inhibition. Levy[54] suggested a more featured PTZ inhibition mechanism which involves regeneration of PTZ in a catalytic cycle. Experimental evidence suggests that disappearance of PTZ is slow. Therefore, the catalytic inhibition mechanism is the main reaction route. The stoichiometric coefficient largely depends on reaction temperature, because at elevated temperature formation of high flux of alkyl radicals significantly increases the side reactions. The mechanism is illustrated in Scheme 3.34.

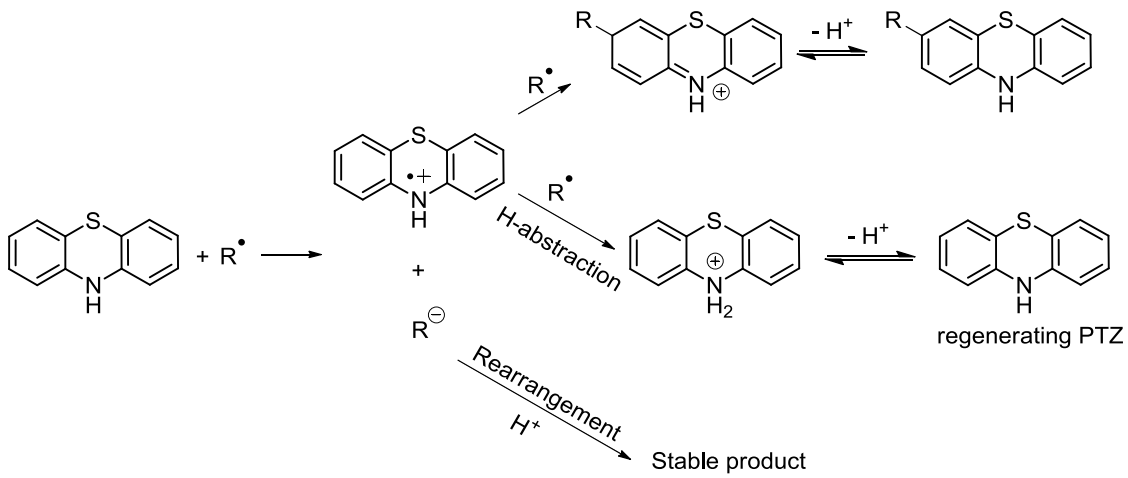

Scheme 3. 34. Catalytical inhibition mechanism of PTZ.

Nitroxide-based inhibitors

Similar to molecular oxygen and PTZ, nitroxide inhibitors (*e.g.* TEMPO) work via reactions with alkyl radicals. Nitroxide radicals terminate the propagation chains via an addition reaction to form a non-radical product (Scheme 3.35). Addition of nitroxide radicals to alkyl radicals (reaction 17) forms stable nitroxyl adduct[55]. This reaction is fast. The rate of the combination of TEMPO with primary alkyl radicals was reported to be *ca.* 10^9 $M^{-1}\cdot s^{-1}$ at 60 ℃.[21] Reaction of nitroxide radicals with alkoxyl radicals is less efficient. Peroxyl radicals do not react with aliphatic nitroxide radicals under neutral conditions.

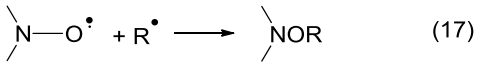

Scheme 3. 35. Inhibition mechanism of nitroxide-based inhibitors.

A recent report suggests[56] that under acidic conditions, TEMPO derivatives can react with peroxyl radicals efficiently. In acid, protonated nitroxide has lower BDE(O-H) than the corresponding hydroxylamine. This makes protonated TEMPO a good hydrogen atom donor which can react with peroxyl radicals. The reaction is shown in Scheme 3.36.

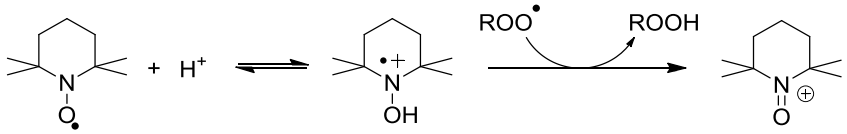

Scheme 3. 36. Reaction of TEMPO with peroxyl radical under acidic conditions.

In the presence of acetic acid, the reaction rate of peroxyl radicals with TEMPO is *ca.* 10^7 $M^{-1}{\cdot}s^{-1}$ at 30 ℃. Therefore, under acidic conditions, TEMPO can quench both alkyl radicals and peroxyl radicals. It makes TEMPO an efficient antioxidant for acidic monomers.

3.1.3. Aims and objectives

The work described in this chapter details the investigation into nitroxide-based inhibitors in a number of organic monomers. Although radical polymerization and its inhibition are very important in industrial applications, the inhibition mechanism is often vague. For instance, the inhibition mechanism of nitroxide-based polymerization inhibitors is often attributed to addition of nitroxide to alkyl radicals or HAT of protonated nitroxide with peroxyl radicals. However, the effect of acid-catalyzed disproportionation of nitroxide radicals is not considered in the inhibition mechanism. Furthermore, practically polymerization inhibitors are commonly used in their mixtures, but the synergism of the inhibitors is unclear. There are a few studies on the interaction of dissolved O_2 and polymerization inhibitors, however, the synergistic inhibition mechanism of the additional inhibitors is not known. Hence, the aim of this investigation was to unveil the mechanism of inhibition and the associated chemistry in nitroxide (*e.g.* TEMPO) inhibited, self-initiated polymerization of acrylic acid. To achieve the aim, an investigation methodology was to be developed to support mechanistic study of TEMPO reactions in organic monomers. The synergistic inhibition mechanism of TEMPO with two common inhibitors, MEHQ and PTZ, was to be studied in acrylic acid. To propose a detailed mechanism of TEMPO derivatives in acrylic acid, a model system was to be built to permit kinetic and mechanistic studies.

3.2. Methodology development for monitoring nitroxide inhibited polymerization

Spontaneous radical polymerization systems involve self-initiation, chain growth and inhibition mechanisms. As discussed in Section 3.1.2.1 (p90), deactivation of the propagation chain can be achieved using three competing termination pathways. Firstly, reaction of alkyl propagation radical with molecular oxygen is rapid and efficient, leading to formation of peroxyl radicals which are much less reactive. However, oxygen inhibited polymerization generates alkoxyl radicals as O_2 depletes, which leads to initiation when O_2 concentration is low. Secondly, alkyl radicals can be terminated by reactions with additional polymerization inhibitors/retarders, either via hydrogen abstraction or an addition reaction, or both. Often a less reactive species or a non-radical product is formed in this mechanism. Thirdly, radical combination and dismutation of the propagation chain leads to termination. Due to the high reactivity of alkyl radicals and the high concentration of unsaturated compounds, the alkyl radicals tend to react with double bonds. Hence this mechanism is less effective for monomers. In summary, inhibition mechanism may mainly rely on quenching propagation radicals with molecular oxygen and with inhibitor (*e.g.* TEMPO). In fact, oxygen is consumed during propagation. Hence, in order to understand the inhibition mechanism of nitroxide radicals, it is necessary to monitor concentrations of both nitroxide inhibitor and oxygen in the system.

3.2.1. Monitoring O_2 concentration

3.2.1.1. Analytical method survey

Measuring dissolved oxygen concentration (DO)[57] is critical for many areas from manufacturing to *in vivo*. This is often achieved by using either a pressure sensor or an oxygen sensor. Monitoring pressure in a closed system involves a pressure transducer and requires a large quantity of sample, therefore not convenient. An alternative means of sensing oxygen have been explored during the last few decades, with developments in oxygen electrodes and optical oximetry methods.

Polarographic (Clark-type)[58-59] and galvanic[60] electrodes are commonly used for measuring DO, but these methods are not suitable for organic media. Optical oximetry employs a fluorescence probe and a fluorescent dye. The DO measurement is based on quenching of fluorescence by oxygen[61-62]. However, fluorescence oximetry depends on the lifetime of the fluorescence probe, therefore is not suitable for DO measurements over a long time range.[63]

Apart from the conventional methods, EPR oximetry[64] is a valuable way to monitor oxygen concentration. In EPR oximetry, DO measurement is based on the interaction of dissolved oxygen molecules and an external paramagnetic species. Applications of EPR oximetry in medicinal and biological chemistry[65-67] have drawn much attention during the past few decades due to its advantage as a minimally invasive, sensitive and accurate method to measure partial oxygen pressure ($p(O_2)$) *in vivo* and *in vitro*. Adoption of this method into organic systems[68] has also shown much potential due to its high sensitivity and minimum sample requirement. Hence, EPR oximetry was employed as a main investigation method in this work.

3.2.1.2. EPR oximetry

EPR oximetry is based on the fact that the EPR linewidth of some paramagnetic species depends on $p(O_2)$. Molecular oxygen, which is a naturally occurring triplet radical, cannot be directly detected by EPR spectroscopy due to its fast relaxation. Therefore, this technique usually employs a second paramagnetic material in the system. Most commonly used probe is soluble persistent free radicals (*e.g.* TEMPO) and paramagnetic solids (*e.g.* fusinite)[69-71]. The external paramagnetic species interacts with molecular oxygen, which broadens its EPR linewidth. Two interactions contribute to the line-broadening effect, Heisenberg spin exchange[72] and dipole-dipole interaction. In dilute solutions, dipolar interaction averages out. For most systems with low viscosity, the exchange interaction dominates and dipole-dipole interaction is negligible. Broadening of the EPR linewidth by O_2 via exchange interaction during its collision with the external paramagnetic species, is proportional to $p(O_2)$ or O_2 concentration. EPR peak-to-peak linewidth is described[73] by equation 3.2.

$$\Delta H_{pp} = \Delta H_{\text{int}} + 4\pi R D_{ox}[O_2] \quad (3.2)$$

Here, ΔH_{pp} is the peak-to-peak EPR linewidth, ΔH_{int} is the intrinsic linewidth, R is the interaction radius between oxygen and the external paramagnetic material, D_{ox} is diffusion coeffecient of oxygen, $[O_2]$ is dissolved oxygen concentration.

Since the line broadening effect is a function of oxygen concentration, quantification of O_2 is possible. Conventionally, instead of the linewidth, peak height of EPR spectra is often measured as a function of oxygen concentration.[73] This method assumes a constant intensity of the paramagnetic material. However, concentration of the paramagnetic material often changes. As a result, this method has a significant limitation when the reporting species is consumed during the measurement.

3.2.2. Methodology development for EPR oximetry

3.2.2.1. Fitting method

Visually, introduction or removal of oxygen into a sample solution leads to reversible EPR linewidth change. For instance, deoxygenation process often results in sharpening of EPR spectra (Figure 3.7).

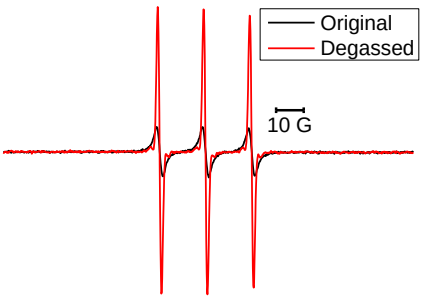

Figure 3. 7. EPR spectra of TEMPO: a, air-saturated (black). b, deoxygenated (red).

Hence, fitting EPR spectra of samples with different oxygen concentration permits measurement of relative and absolute $[O_2]$ in such systems.

The assumption of the conventional peak height measurement is that intensity of the reporting radical does not change during the process. Evidently this method has a profound limitation as concentration of the external paramagnetic material is not constant in many cases. Smirnov[74] *et al.* developed a convolution-based fitting method to extract the line broadening function from the EPR line shapes by fitting experimental spectra as a convolution of an unbroadened EPR spectrum (normally obtained from a deoxygenated sample) and a Lorentzian[72] function. The fitting result can either be presented as a line broadening function or can be transformed into concentration units. If only relative oxygen concentration is of interest, an alternative fitting against a simulated sharp spectrum is also valid. This fitting method has been used in many biological systems, but few applications are reported in organic systems.

3.2.2.2. EPR oximetry via convolution-based fitting method

We thus adopted the oximetry fitting method in the investigation of organic polymerization systems. To study the inhibition mechanism of TEMPO derivatives in acrylic acid, kinetic profiles of both nitroxide and oxygen consumption are important. This method has a significant advantage as it allows simultaneous determination of both TEMPO and O_2 concentrations. Besides, the fitting method also gives more accurate results compared to the conventional peak height measurement method. Fitting of experiment spectra utilizes all data points, while the conventional method usually relies on only two points.

To establish the feasibility of using this fitting method in organic systems, a deoxygenation experiment was carried out. An air saturated solution of 20ppm TEMPO in distilled acrylic acid was sealed in a gas-permeable Teflon tube and deoxygenated in an N_2 flow at room temperature. EPR spectra of TEMPO in acrylic acid were recorded over *ca.* 1.5 hours. Figure 3.8 shows EPR spectra linewidth plotted against time, which could also be interpreted as evolution of oxygen concentration in the solvent. A clear linewidth sharpening effect was observed, which is consistent with the deoxygenation process.

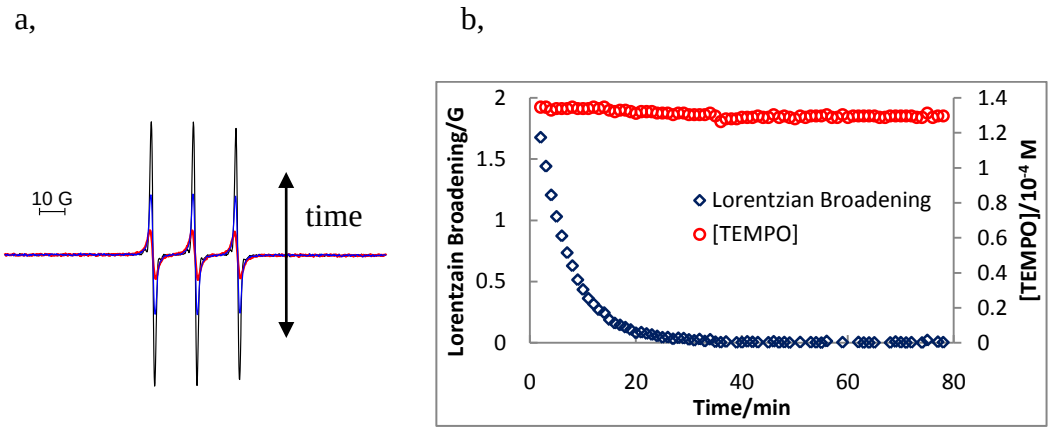

Figure 3. 8. Deoxygenation by blowing N_2 gas through a solution of 20ppm TEMPO in acrylic acid sealed in an oxygen-permeable Teflon tube: a, EPR spectra of TEMPO at 0 (red), 5 (blue) and 20 (black) minutes of the deoxygenation process. b, time evolution of Lorentzian broadening (◊) and [TEMPO] (○) using completely deoxygenated sample as a reference.

To establish the methodology in a real polymerization system, TEMPO inhibited, spontaneous polymerization of styrene was studied as a model system[68]. Upon heating 40ppm TEMPO in distilled styrene solution sealed in a capillary in the EPR cavity at 100 ℃, sharpening of EPR spectra was observed over time as a result of the autoxidation process of styrene. As shown in scheme 3.22 (p92), Diels-Alder self-reaction of styrene leads to formation of a carbon-centred radical which reacts with dissolved oxygen rapidly. Oxygen consumption results in sharpening of TEMPO EPR spectra. The series of spectra were fitted and a time dependence of oxygen and TEMPO concentration is shown in Figure 3.9.

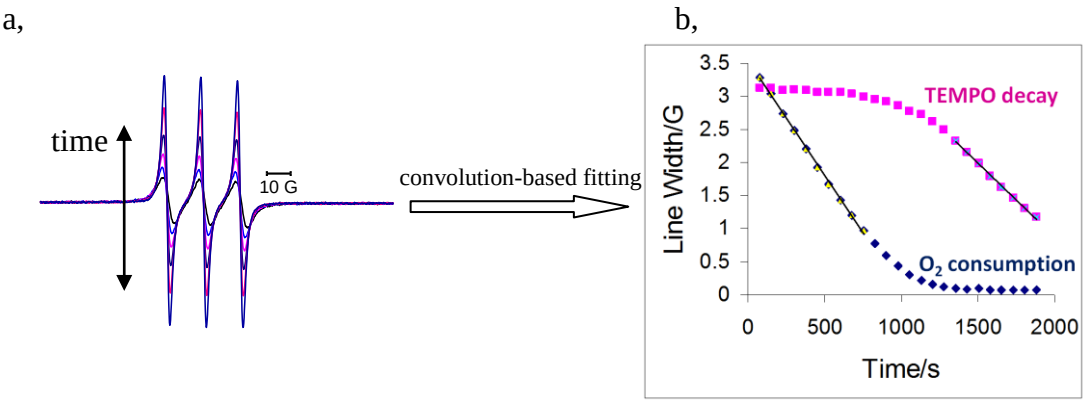

Figure 3. 9. TEMPO EPR signal evolution in distilled styrene in a sealed capillary at 100 ℃. A convolution-based fitting method was used to simultaneously determine both TEMPO decay

and oxygen consumption. a, EPR spectra of TEMPO at different times. b, time evolution of TEMPO intensity (pink) and Lorenzian line broadening (blue).

Figure 3.9 shows that while oxygen was being consumed in the reaction, TEMPO concentration remained relatively stable. After oxygen was consumed, TEMPO started to decay rapidly. This observation confirms the commonly accepted mechanism of nitroxide polymerization inhibitors[21, 75]. In the beginning, oxygen reacts with alkyl radicals fast to form peroxyl radicals, which results in consumption of oxygen. Nitroxide radicals also react with the propagation radicals but the reaction rate is slower than for oxygen. Peroxyl radicals do not react with TEMPO. Therefore, in the beginning of the reaction, nitroxide concentration stays relatively unchanged. As oxygen is consumed, TEMPO starts to act as a major inhibitor to quench alkyl radicals. This mechanism shows that nitroxide radical inhibitors remain active when oxygen concentration is low.

3.2.3. Oximetry fitting method in nitroxide inhibited methyl methacrylate and acrylonitrile

The results obtained in TEMPO inhibited spontaneous polymerization of styrene demonstrated the useful application of the oximetry fitting method. In order to further validate the methodology and test the scope of its application, the oximetry fitting method was used to study the TEMPO inhibited spontaneous polymerization of methyl methacrylate and acrylonitrile. As discussed in Section 3.1.1.3 (p86), a TEMPO derivative, 4-hydroxy-TEMPO (4HT) is widely used commercially as a polymerization inhibitor. It is mainly used to stabilize styrene, methyl methacrylate, acrylonitrile and acrylic acid (Figure 3.10).

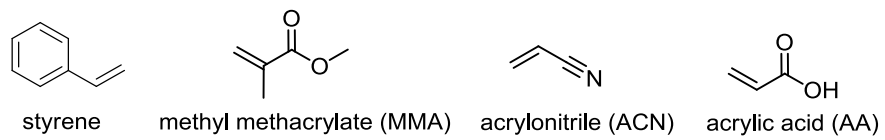

Figure 3. 10. Structures of styrene, methyl methacrylate, acrylonitrile and acrylic acid.

Figure 3.5 (p89) shows an inhibition efficacy study of 4HT in spontaneous methyl methacrylate polymerization. It suggested that as soon as 4HT was introduced to methyl methacrylate polymerization mixture, polymerization stopped immediately. However, the efficacy study did not provide kinetic data for 4HT decay and oxygen consumption.

3.2.3.1. 4HT inhibited spontaneous polymerization of methyl methacrylate and acrylonitrile

In order to generate kinetic data, a solution of 100ppm 4HT in neat methyl methacrylate was sealed in a capillary. The capillary was heated at 100 ℃ inside an EPR cavity to stimulate autoxidation. As shown in Figure 3.11, after prolonged heating (16 hours) of the reaction mixture, 4HT concentration remained constant while relative oxygen concentration dropped significantly. Surprisingly 4HT decay was not observed on this time scale.

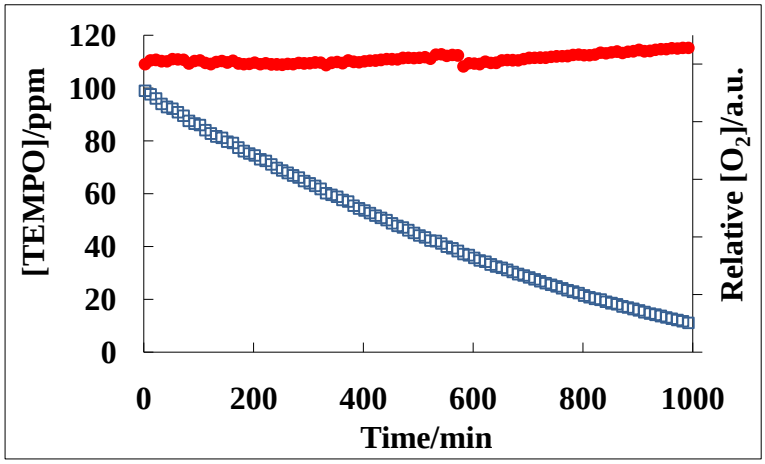

Figure 3. 11. 100ppm 4HT (5.47×10^{-4} M) inhibited spontaneous polymerization of methyl methacrylate in a sealed capillary at 100 ℃: Time-dependent decay of 4HT (red) and oxygen (blue).

Presumably as oxygen concentration becomes lower, 4HT decay would occur upon further heating. But compared to the observations in styrene, where TEMPO is consumed within 0.5 h, spontaneous polymerization of methyl methacrylate is significantly slower. A lack of efficient initiation mechanism could explain this effect. In styrene, the Mayo mechanism provides an effective route for generating

alkyl radicals. In methyl methacrylate, it is speculated that the self-initiation process largely relies on thermal initiation (Scheme 3.23, p92), hydrogen abstraction by oxygen species (Scheme 3.26-3.28, p93-94) and impurities such as peroxides (Scheme 3.24, p93) and metal salts (Scheme 3.25, p93). Therefore, the O_2 consumption in methyl methacrylate is much slower than in styrene, which leads to a stable 4HT concentration.

A similar observation was obtained in acrylonitrile (Figure 3.12). Upon heating 100ppm 4HT in neat acrylonitrile in a sealed capillary at 100 ℃, a significant drop of relative oxygen concentration was obtained. However, in the time scale of 13 hours, 4HT concentration dropped by only 10%. Similarly, it's plausible to presume that more aggressive 4HT decay would occur eventually upon further heating.

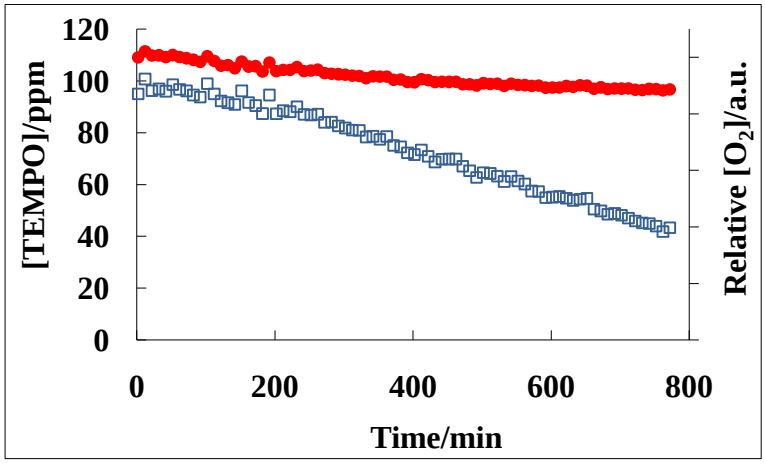

Figure 3. 12. 100ppm 4HT (4.71×10^{-4} M) inhibited spontaneous polymerization of acrylonitrile in a sealed capillary at 100 ℃: Time-dependent decay of 4HT (red) and oxygen (blue).

In summary, self-initiation rate of styrene is much faster than methyl methacrylate and acrylonitrile. It suggests that Mayo mechanism is the primary route of styrene autoxidation process. In methyl methacrylate and acrylonitrile, there is no effective self-initiation mechanism. The oximetry fitting method showed reproducibility in different polymerization systems. However, the instrument stability limits the use of this method to monitor long reactions (*e.g.* reactions which last for days).

3.2.4. Methodology limitations

During the work on the feasibility of EPR oximetry, some limitations of the fitting methodology were noticed. Firstly, in an extremely slow self-initiated polymerization process, the reaction time is so long that stability issue of the EPR instrument may be no longer negligible. In Figure 3.11 (p106), one can see a break point in the kinetic curve of oxygen consumption. After carefully examining the original spectra, it was confirmed that phase instability was responsible for this observation. Although phase was corrected during the fitting process, a phase change which occurs suddenly in the series of spectra results in different total intensity and becomes a source of error. It is possible to increase the reaction rate considerably by carrying out these experiments at a higher temperature. In industry, the temperature of polymerization reactors[29] of acrylonitrile ranges from 60-150 ℃. The temperature of methyl methacrylate reactors is even higher. However, the boiling points of methyl methacrylate and acrylonitrile are 101 ℃ and 77 ℃, respectively. Overheating the samples may risk an explosion inside the EPR spectrometer. Therefore, the first limitation of this methodology is that it is difficult to monitor slow reactions which require substantial reaction time.

Secondly, accuracy of such measurements largely depends on the quality of fitting. It has been noticed that the fitting software cannot cope with the small linewidth of the broadening function. Therefore, if oxygen consumption leads to very sharp EPR spectra which are comparable to that of the reference sample (*e.g.* completely deoxygenated sample), the fitting becomes less accurate or even fails in some cases. Fortunately, this problem can be easily solved. It is possible to manually simulate a sharper EPR spectrum by manipulating the linewidth parameters. This artificial spectrum is much sharper than experimental spectra. By using the simulated spectrum as a reference, adequate linewidth differences allow proper fitting performance. Consequently, an accurate kinetic analysis can be achieved.

Thirdly, EPR oximetry relies on the external paramagnetic species. In this case, nitroxides are the reporting material in the system. The advantage of EPR oximetry in studying nitroxides inhibited polymerization is that the concentration of nitroxides is also of primary interest in the investigation. However, when nitroxides

concentration becomes too low, it could jeopardize the reliability of this method. In industrial conditions, several tens ppm of nitroxide concentration is a typical value used for storage of monomers. Sensitivity is in fact an advantage of EPR spectroscopy, but even so, when nitroxide concentration drops significantly below 10ppm, the noise level of EPR spectra starts to affect the fitting quality. In such cases, it was observed that kinetic curve of oxygen consumption became noticeably more scattered. Hence, in this work, higher nitroxide concentration (*e.g.* 100ppm) is often used to allow accurate oxygen consumption measurements.

In conclusion, the limitations of the methodology are mainly difficulties in accurate measurements under some extreme conditions. But overall, this method brings some unique advantages in studying nitroxide inhibited polymerization systems.

3.3. Investigation of spontaneous polymerization of acrylic acid inhibited by nitroxide radicals

3.3.1. Introduction

Acrylic acid (AA) is the simplest unsaturated carboxylic acid. It is an important chemical intermediate used to produce homo- and co-polymers, textiles, and numerous other industrial and consumer products. Wide applications from paints and polishes to plastic and coatings make acrylic acid an extremely valuable product in industry. Modern acrylic acid production is often via gas phase catalytic oxidation of propylene[76] (Scheme 3.37).

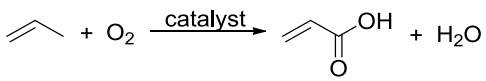

Scheme 3. 37. Catalytic oxidation of propylene to form acrylic acid.

Due to the commercial value of this product, many attempts were made on optimizations of acrylic acid plants. Even so, temperature of acrylic acid reactor is

usually still very high (200-300 ℃). As discussed in Section 3.1.2.2 (p91), spontaneous polymerization can be initiated by impurities in the plant or other self-initiation mechanism. Primary radicals ($R^{\bullet}$) formed in the initiation step can add to the vinyl group on acrylic acid resulting in formation of the propagation radical (Scheme 3.38).

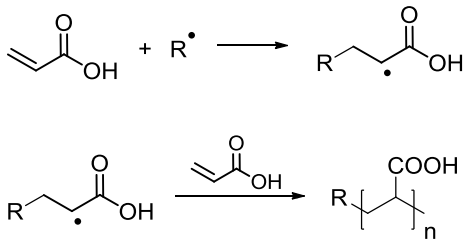

Scheme 3. 38. Radical polymerization of acrylic acid.

Common inhibitors used in acrylic acid include 4-hydroxy-TEMPO (4HT), 4-methoxyphenol (MEHQ) and phenothiazine (PTZ). As discussed in Section 3.1.2.3 (p94), these stabilizers have different inhibition mechanisms. In fact, stabilizer mixtures are commonly used in monomers to achieve a synergistic and enhanced inhibition effect. However, the synergistic mechanism of inhibitor mixtures is not clearly known. Therefore, in this work particular attention was paid to the chemistry of nitroxide-containing inhibitor mixtures in spontaneous polymerization of acrylic acid. The study was carried out using EPR oximetry via convolution-based fitting method.

3.3.2. Investigation of synergistic inhibition of self-initiated acrylic acid polymerization

3.3.2.1. Inhibition of self-polymerization of acrylic acid by 4HT/MEHQ and 4HT/PTZ mixtures

The inhibition effect of 4HT/MEHQ and 4HT/PTZ mixtures were studied due to their extensive application in industry, but more importantly, because of their different inhibition mechanism. MEHQ is known to inhibit propagation by intercepting peroxyl radicals and slowing down oxygen consumption, but it is not

efficient in quenching alkyl radicals. 4HT and PTZ both work by reacting with alkyl radicals but not efficient in trapping peroxyl radicals. Effectively, 4HT/MEHQ is a mixture of different types of inhibitors, and 4HT/PTZ is a mixture of the same type of inhibitors.

Therefore mixtures of 4HT with MEHQ and PTZ were heated in acrylic acid to high temperature (*e.g.* 100 ℃) to monitor 4HT and oxygen concentration using EPR oximetry. Surprisingly, we observed that in acidic media, the presence of PTZ significantly accelerated 4HT decay. Figure 3.13 shows that, in the presence of 100ppm PTZ, 100ppm 4HT decays very fast in acrylic acid even at room temperature. This effect was not observed in neutral monomers (*e.g.* styrene). Due to the low 4HT concentration, oxygen concentration obtained from the oximetry fitting method showed significant scattering. However, it is clear that relative $[O_2]$ does not change, which can be explained by lack of self-initiation of acrylic acid at room temperature.

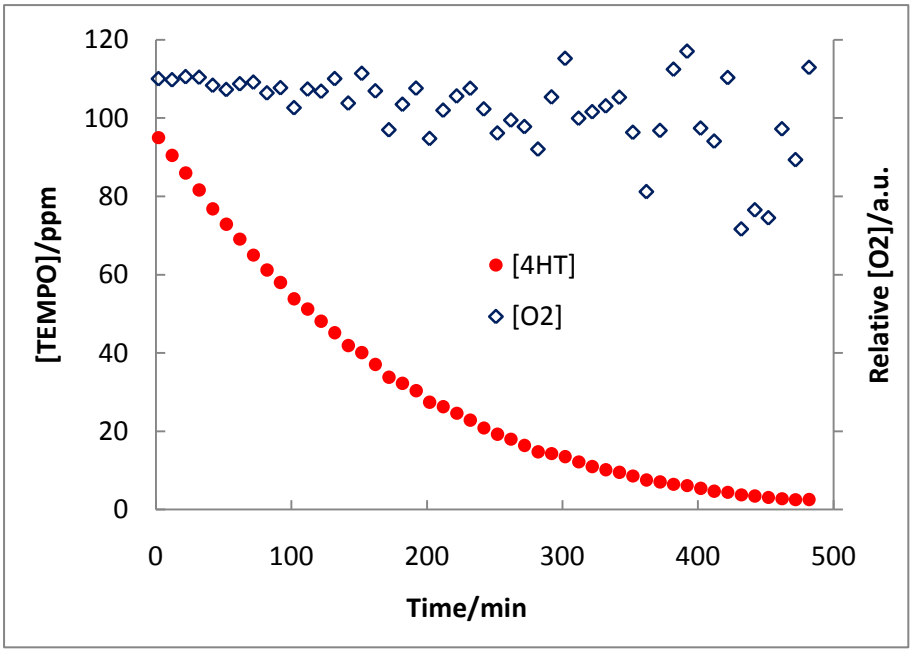

Figure 3. 13. Time-dependent decay of 4HT (●) and oxygen (◊) in an acrylic acid solution of 100ppm 4HT (6.10×10^{-4} M) and 100ppm PTZ (5.27×10^{-4} M) mixture at room temperature.

This interesting observation is likely to be a result of oxidation of PTZ by oxoammonium salt which is a product of 4HT disproportionation reaction (Scheme

3.39). Scheme 3.8 (p81) shows that following protonation of TEMPO derivatives, a disproportionation reaction takes place and yields the corresponding hydroxylamine and *N*-oxoammonium cation. As a strong oxidizing agent, oxoammonium salt can oxidize PTZ to its radical cation and be reduced to nitroxide radical.[77] The PTZ radical cation can be further reduced to form a divalent ion. Consumption of oxoammonium salt drives the 4HT disproportionation reaction to completion.

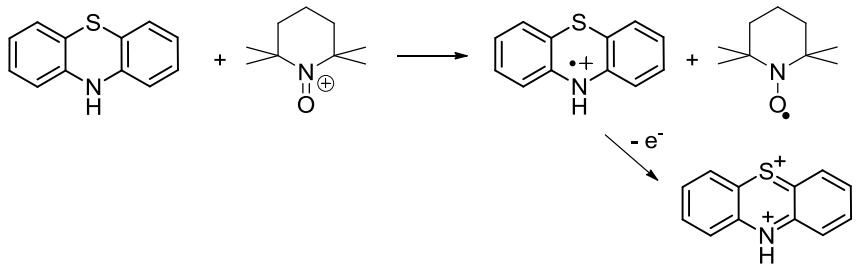

Scheme 3. 39. Oxidation of PTZ to its radical cation by oxoammonium salt.

At high temperature (*e.g.* 373K), decay of 4HT is too fast to be monitored by EPR in the presence of PTZ. In order to slow down 4HT decay, a much lower concentration of PTZ (10ppm) was used to allow proper kinetic investigations.

Therefore, a solution of 100ppm 4HT and 10ppm PTZ in distilled acrylic acid was sealed in a small capillary. The capillary was heated inside EPR cavity at 100 ℃ and EPR spectra were recorded over time. Similarly, the 100ppm 4HT alone and a mixture of 100ppm 4HT with 100ppm MEHQ in acrylic acid was also monitored at 100 ℃ using the same approach. Analysis of EPR spectra provides kinetic profiles of 4HT decay and O_2 consumption (Figure 3.14).

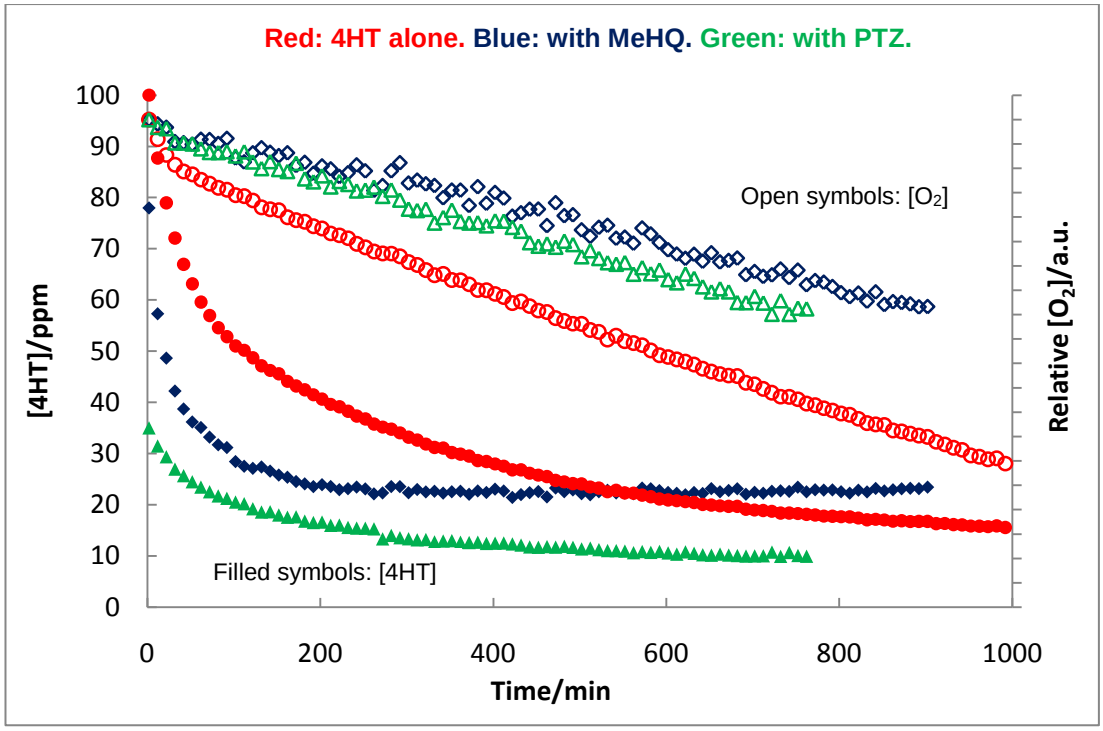

Figure 3. 14. Red: [4HT] (●) and relative [O_2] (○) decay of 100ppm 4HT in acrylic acid at 100 ℃. Blue: [4HT] (♦) and relative [O_2] (◊) decay of 100ppm 4HT + 100ppm MEHQ in acrylic acid at 100 ℃. Green: [4HT] (■) and relative [O_2] (□) decay of 100ppm 4HT + 10ppm PTZ in acrylic acid at 100 ℃.

As shown in Figure 3.14, oxygen consumption in 4HT inhibited acrylic acid is much slower as compared to in styrene (Figure 3.9, p104). It suggests that in acrylic acid, there is no efficient self-initiation mechanism. Oxygen consumption in acrylic acid inhibited by 4HT/MEHQ mixture is slower than inhibited by 4HT alone. This observation is different as compared to styrene[68]. In styrene, presence of MEHQ accelerates oxygen consumption. We have proposed a mechanism to explain this observation (Scheme 3.40). Hydrogen atom hopping between TEMPO and MEHQ leads to a dynamic equilibrium of phenoxyl radical and TEMPO. The phenoxyl radical can abstract the labile hydrogen from the dimerization product of styrene Diels-Alder self-reaction. This reaction yields high flux of alkyl radicals and induces accelerated oxygen consumption. Hydrogen abstraction from MEHQ by TEMPO is not favourable due to the bond dissociation energies of TEMPOH and MEHQ (Table 3.1, p82). The reaction is driven by hydrogen abstraction from styrene dimer by the phenoxyl radical to form an aromatic compound.

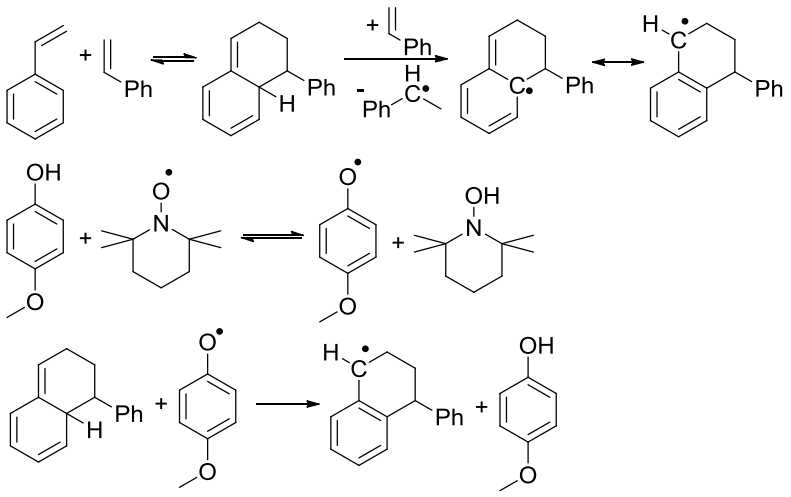

Scheme 3. 40. Anti-synergistic inhibition mechanism of TEMPO and MEHQ in styrene autoxidation process

In acrylic acid, the driving force for this mechanism does not exist. Therefore, low concentration of phenoxyl radicals, which are not effective in adding to double bonds, cannot promote alkyl radical formation. Quenching peroxyl radicals by MEHQ is the main reaction route, and thus slows down oxygen consumption.

For 4HT/PTZ inhibited polymerization of acrylic acid, the presence of 10ppm PTZ also decelerates oxygen consumption considerably. PTZ inhibits chain propagation via reactions with alkyl radicals. Its reaction with peroxyl radicals is not efficient. Therefore, slower oxygen consumption in this experiment is not due to PTZ alone, but hydroxylamine. The role of hydroxylamine is discussed later in detail in Section 3.3.2.2 (p115).

Interestingly, 4HT decay in its mixtures with MEHQ and PTZ is very different to 4HT alone. In the presence of MEHQ, 4HT decay reaches an equilibrium state so that a lower concentration of 4HT is maintained while oxygen continues to deplete in this system (Figure 3.14, blue, p113). One possible explanation is via hydrogen abstraction from hydroxylamine by MEHQ phenoxyl radical (Scheme 3.41). MEHQ reacts with peroxyl radicals leading to accumulation of phenoxyl radicals (reaction 14). Large amount of phenoxyl radicals abstract hydrogen atoms from 4HT hydroxylamine, leading to formation of 4HT back again (reaction 18).

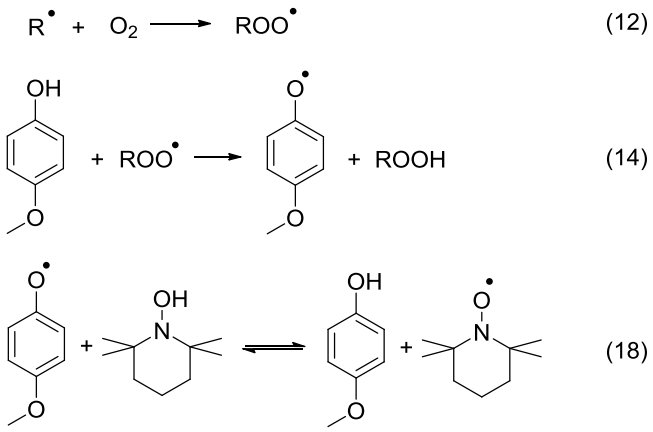

Scheme 3. 41. Proposed mechanism of synergistic inhibition effect of MEHQ and TEMPO hydroxylamine.

On the contrary, 4HT decay is significantly accelerated by PTZ. Particularly at high temperature, in the presence of equivalent amount of PTZ, 4HT decays so fast that 4HT EPR signal disappears within 20 minutes. However, 4HT/PTZ mixture is still effective in inhibiting chain propagation. Decay of 4HT is due to oxidation of PTZ by oxoammonium salt formed in the disproportionation of 4HT (Scheme 3.39, p112). PTZ radical cation is formed in this reaction, which inhibits polymerization. In the mean time, oxoammonium cation was reduced back to TEMPO derivatives which can undergo disproportionation reaction to yield hydroxylamine and oxoammonium cation. This reaction leads to accumulation of the corresponding hydroxylamine. Since 4HT and PTZ are consumed in the reaction with each other, it would be reasonable to assume that the reaction interferes with the inhibition effect. However, it is not the case according to industrial practice. One major product in this system is hydroxylamine which can also act as a hydrogen donor. The effect of hydroxylamine in the inhibition mechanism is likely to be significant. Therefore, the role of hydroxylamine in spontaneous polymerization of acrylic acid was studied and discussed in next section.

3.3.2.2. The effect of hydroxylamine on the inhibition mechanism of 4HT in self-polymerization of acrylic acid.

In order to establish the role of hydroxylamine on the inhibition mechanism, a solution of 100ppm 4HT and 100ppm of the corresponding hydroxylamine in

distilled acrylic acid was sealed in a capillary and heated inside EPR cavity at 100 ℃. EPR spectra recorded over time were analyzed using the oximetry fitting method. 4HT decay and oxygen consumption are shown in Figure 3.15.

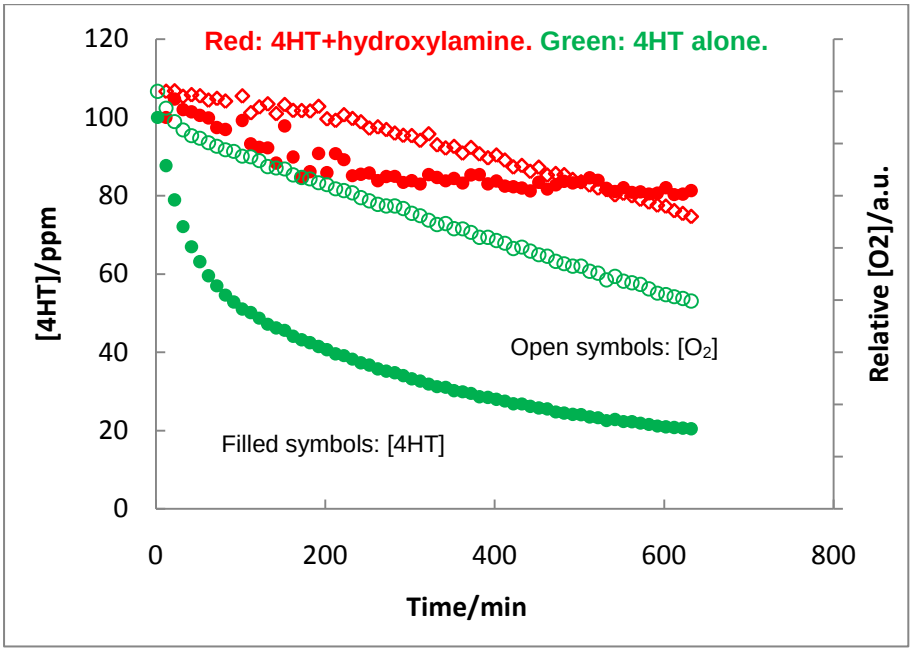

Figure 3. 15. Red: 4HT (●) and oxygen (◊) concentration of an acrylic acid solution of 100ppm 4HT + 100ppm 4HT hydroxylamine at 100 ℃. Green: 4HT (●) and oxygen (◊) decay of an acrylic acid solution of 100ppm 4HT at 100 ℃.

4HT decay is slowed down significantly in the presence of 4HT hydroxylamine. Oxygen consumption is also slower. Reaction of hydroxylamine with alkyl radicals and peroxyl radicals could explain this observation (Scheme 3.42). Hydrogen abstraction from hydroxylamine by alkyl and peroxyl radicals regenerates nitroxide radicals, which explains the slow 4HT decay. Similar to the inhibition mechanism of MEHQ, interception of peroxyl radical by hydroxylamine via hydrogen abstraction leads to stable hydroperoxides ROOH (reaction 20). The reaction decelerates oxygen consumption. As compared with the effect of 4HT alone and 4HT/MEHQ mixture, the result indicates that interception of peroxyl radicals by hydroxylamine is more efficient than by nitroxide radicals but not as good as MEHQ.

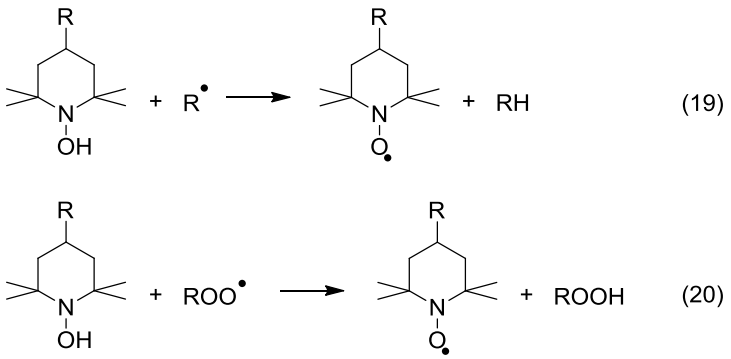

Scheme 3. 42. Reactions of hydroxylamine with alkyl and peroxyl radicals.

This mechanism also explains the slower oxygen consumption in 4HT/PTZ inhibited acrylic acid (Section 3.3.2.1, Figure 3.14, p113). Oxidation of PTZ by oxoammonium cation leads to regeneration of nitroxide radicals, which then undergo disproportionation reaction. The whole mechanism leads to accumulation of hydroxylamine. We have identified the effect of hydroxylamine in slowing down oxygen consumption and reforming 4HT. Hydroxylamine reacts with peroxyl radicals and consequently decelerates oxygen consumption. Therefore, we have proposed a synergistic inhibition mechanism for TEMPO/PTZ in acrylic acid (Scheme 3.43).

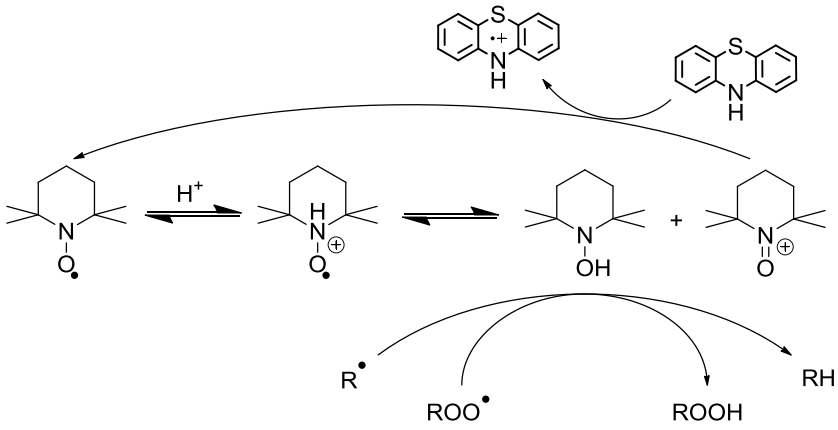

Scheme 3. 43. Inhibition mechanism of 4HT/PTZ mixture in acrylic acid self-polymerization.

3.3.3. Mechanistic study on 4HT in self-polymerization of acrylic acid

Synergism of nitroxide with other types of polymerization inhibitors showed complex mechanism in acrylic acid. Developing detailed inhibition mechanisms

requires better understanding of the chemistry of nitroxide in acidic monomers. Hence, 4HT inhibited spontaneous polymerization of acrylic acid was studied. A solution of 100ppm 4HT in distilled acrylic acid was sealed in a capillary. The capillary was heated at 100 ℃ inside EPR cavity to initiate spontaneous polymerization. As shown in Figure 3.16, EPR signal intensity dropped significantly during the test. Data analysis by the fitting method, revealed substantial 4HT decay as well as O_2 consumption. On one hand, oxygen consumption is much slower than in styrene (Figure 3.9, p104) due to a lack of efficient self-initiating mechanism. On the other hand, unlike in the neutral monomers, 4HT concentration drops quickly in the beginning of the reaction.

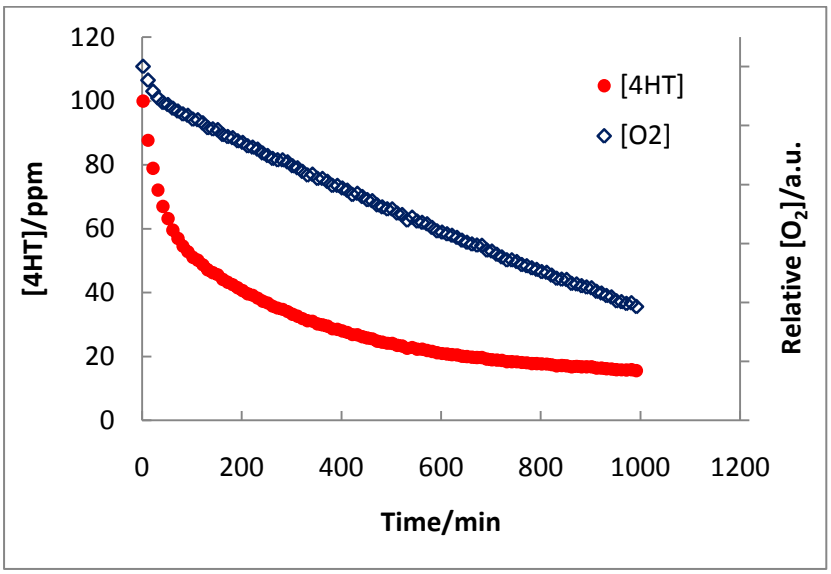

Figure 3. 16. 4HT (●) and relative oxygen (◊) concentration decay of an acrylic acid solution of 100ppm 4HT.

Rapid decay of 4HT in spontaneous polymerization of acrylic acid is unclear. Although protonated TEMPO derivatives can react with peroxyl radicals at diffusion controlled rate, the amount of protonated 4HT in acrylic acid is far too small to result in rapid 4HT disappearance. It is therefore likely that acid catalyzed nitroxide disproportionation is responsible for the 4HT decay in this reaction. As shown in Scheme 3.8 (p81), TEMPO derivatives can be protonated in acid. The reaction is followed by disproportionation to yield the corresponding hydroxylamine and *N*-oxoammonium salt. Hydroxylamine has a significant effect on the inhibition mechanism as it can react with alkyl and peroxyl radicals.

In order to understand the effect of solvent, the reactivity of 4HT was also monitored in 50% (w/w) acrylic acid aqueous solution. The pK_a of acrylic acid is 4.25. 50% aqueous acrylic acid (w/w) has a pH of 0.35. Similarly to the previous studies, a solution of 100ppm 4HT in 50% aqueous acrylic acid (w/w) was sealed in a capillary which was heated at 100 ℃ in the EPR cavity. As shown in Figure 3.17, 4HT gave similar intensity decay as in pure acrylic acid. The line width was sharper than in pure acrylic acid because oxygen solubility is lower in aqueous solution than in pure organic media. The result suggests that 4HT decay and oxygen consumption in acrylic acid is a general effect.

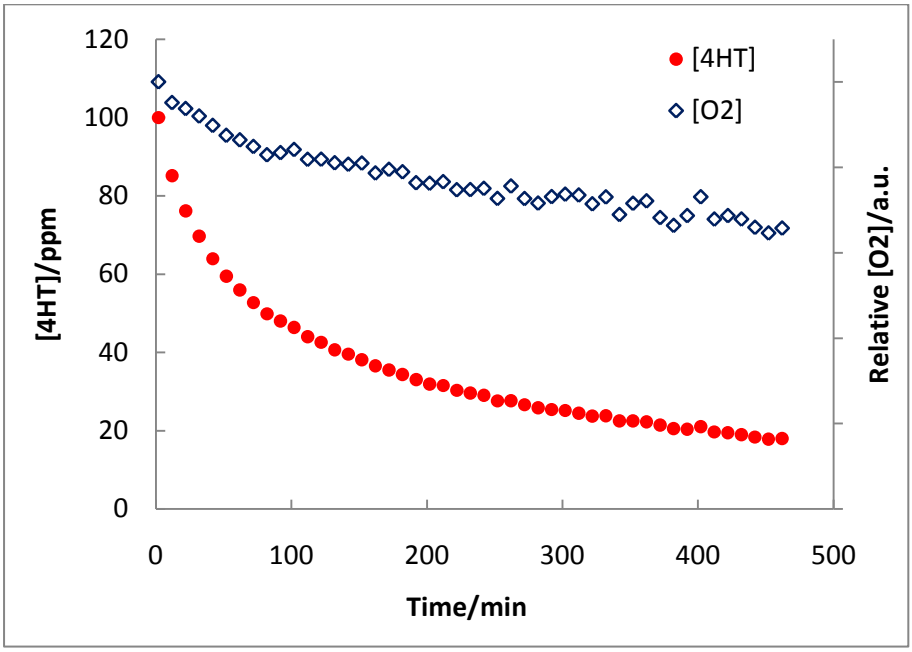

Figure 3. 17. 4HT (●) and oxygen (◊) decay of a 50% aqueous acrylic acid solution of 100ppm 4HT at 100 ℃.

This result gives rise to the question whether disproportionation reaction affects the inhibition mechanism. Therefore, kinetic studies on decay of TEMPO derivatives in acrylic acid were carried out to achieve a better understanding of their inhibition mechanism and associated chemistry. The work is described in Section 3.4 (p121).

3.3.4. Conclusions on mechanistic investigation of inhibited spontaneous polymerization of acrylic acid

Nitroxide radicals and nitroxide containing inhibitor mixtures were studied using EPR oximetry to establish their inhibition mechanism in spontaneous polymerization of acrylic acid. Self-initiation in acrylic acid is not efficient as compared to styrene. The key reaction responsible for the synergistic chemistry of nitroxide/MEHQ mixture is the reversible hydrogen abstraction between nitroxide and MEHQ. Nitroxide radicals react with alkyl radicals rapidly while MEHQ quenches peroxyl radicals efficiently. The equilibrium between nitroxide radical/MEHQ and hydroxylamine/phenoxyl radical provides the utility to inhibit polymerization in the presence and absence of dissolved oxygen.

The mechanism of nitroxide/PTZ inhibited spontaneous polymerization of acrylic acid is more complicated. Fast decay of nitroxide radicals in the presence of PTZ indicates the importance of hydroxylamine in the inhibition mechanism. Disproportionation of nitroxide radicals and oxidation of PTZ by oxoammonium salt leads to a major product in the system – hydroxylamine. Hydroxylamine quenches both alkyl and peroxyl radicals, thus inhibits the propagation and decelerates oxygen consumption.

Nitroxide radical intensity decay in acrylic acid is due to acid-catalyzed disproportionation reaction. The simultaneously observed oxygen consumption was used to assess inhibitor efficacy in the studies of the synergistic inhibition effect. Cooperativity can explain the complicated kinetic profiles but the effect of disproportionation on the inhibition mechanism is not clear. Detailed kinetic studies of nitroxide radical decay in acidic media is necessary to understand the chemistry of nitroxide in spontaneous polymerization of acrylic acid.

3.4. Kinetic and mechanistic investigations of acid-catalyzed TEMPO disproportionation

3.4.1. Introduction

When 4HT decay and oxygen consumption were studied in acidic monomers (*e.g.* acrylic acid), it was noticed that 4HT intensity decayed fast from the beginning. It is likely that the known reaction of acid catalyzed TEMPO disproportionation is responsible for this effect. However, kinetic data of TEMPO disproportionation reaction at high temperature was not established. In order to assist mechanistic investigations, TEMPO decay was studied at high temperature.

TEMPO derivatives can be protonated in acid and further disproportionate to form the corresponding hydroxylamine and oxoammonium salt. Oxoammonium salt is a strong oxidizing agent. Oxoammonium salt oxidizes the 4-hydroxyl group of 4HT to form 4-oxo-TEMPO (Scheme 3.44). This further complicates the reaction.

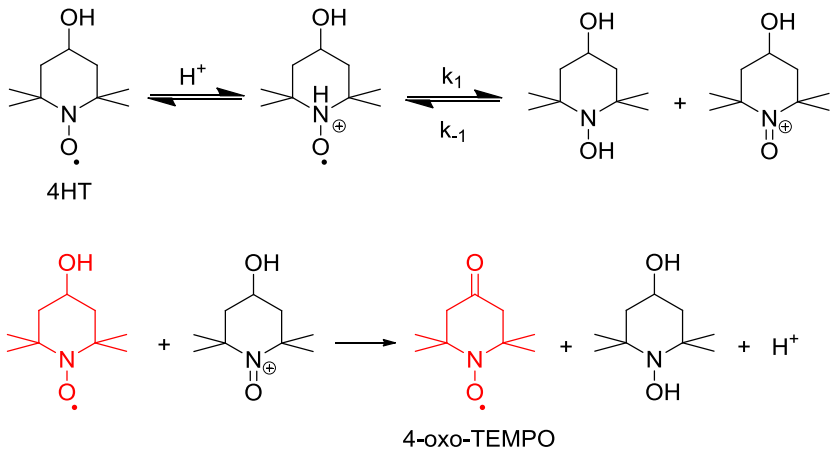

Scheme 3. 44. Acid catalyzed 4HT disproportionation and oxidation of 4HT to 4-oxo-TEMPO by *N*-oxoammonium cation

3.4.2. Kinetic study of acid-catalyzed TEMPO disproportionation

3.4.2.1. The role of substituent in the 4-position

In the 4HT decay in acid, *N*-oxoammonium cation oxidizes 4HT to form 4-oxo-TEMPO (4OT), which leads to a mixture of 4HT and 4OT in the system. If disproportionation rates of 4OT and 4HT are significantly different, the kinetic studies will be further complicated due to this reaction. Therefore, it is important to assess the rate of disproportionation of such TEMPO derivatives. Hence, acrylic acid solutions of 100ppm TEMPO, 4HT, and 4OT were sealed in capillaries, heated at 100 ℃ and monitored by EPR spectroscopy. Thus, nitroxide radical intensity decay was obtained by analyzing the spectra using the oximetry fitting method (Figure 3.18).

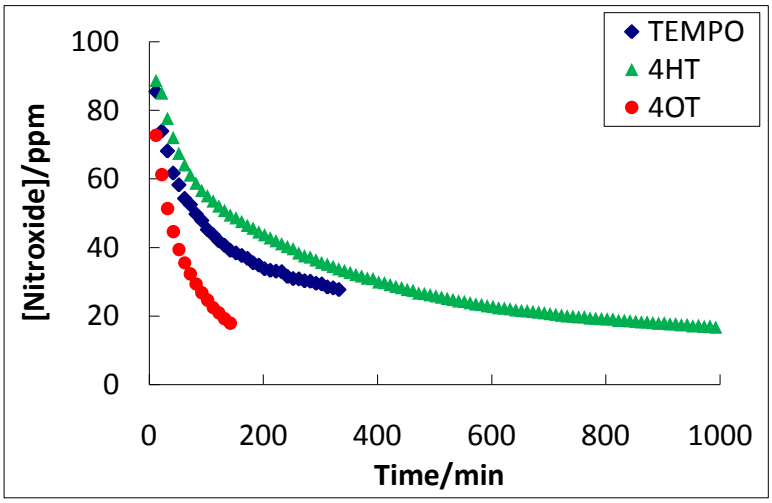

Figure 3. 18. Decay of 100ppm TEMPO (blue), 4HT (green) and 4OT (red) in acrylic acid at 100 ℃.

As shown in Figure 3.18, the decay of 4OT is much faster than TEMPO and 4HT. The origin of this effect is not clear, but it can be tentatively explained by the differences of TEMPO, 4HT and 4OT on the inversion of the piperidine ring. More importantly, the different reaction rate of 4HT and 4OT complicates the kinetic study. Furthermore, the decay of these derivatives does not appear to follow 2nd order kinetic model. In order to simplify the model system, TEMPO was used to undertake the kinetic and mechanistic investigation instead of 4HT.

3.4.2.2. TEMPO disproportionation in acrylic acid

In TEMPO inhibited spontaneous polymerization of styrene, TEMPO decay was observed when the rate of oxygen consumption slowed down. As shown in Figure 3.9 (p104), in the region that oxygen depletion appears to be zeroth order, TEMPO concentration remained constant. In comparison, in nitroxide inhibited spontaneous polymerization of acrylic acid, the psedo-0th order oxygen depletion was only observed on the time scale of our investigation (Figure 3.14 - 3.17). It suggests that the nitroxide decay was primarily due to disproportionation.

We simulated the kinetic profile as an equilibrium using a 2nd order model. TEMPO decay in acrylic acid at 100 ℃ showed a good fit to 2nd order kinetics in the first part of the profile. Afterwards, a deviation from 2nd order was observed (Figure 3.19).

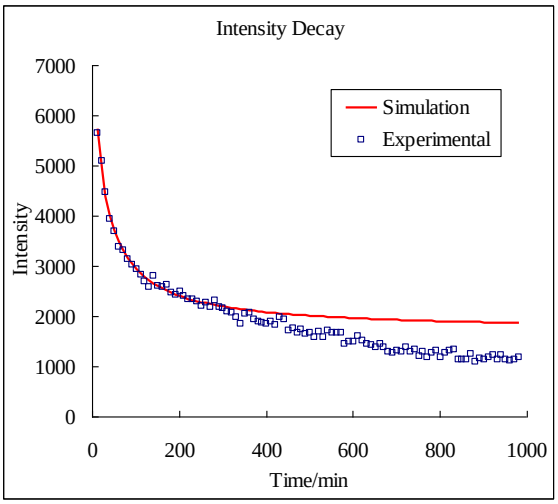

Figure 3. 19. Experimental data and 2nd order kinetic fitting of 100ppm TEMPO in acrylic acid at 100 ℃.

In order to build a kinetic model of TEMPO consumption, TEMPO decay in acrylic acid starting with various concentrations/mass ratio (*e.g.* 1%, 0.1%, 100ppm, 40ppm, 20ppm, 10ppm) was studied. The kinetic profiles are shown in Figure 3.20.

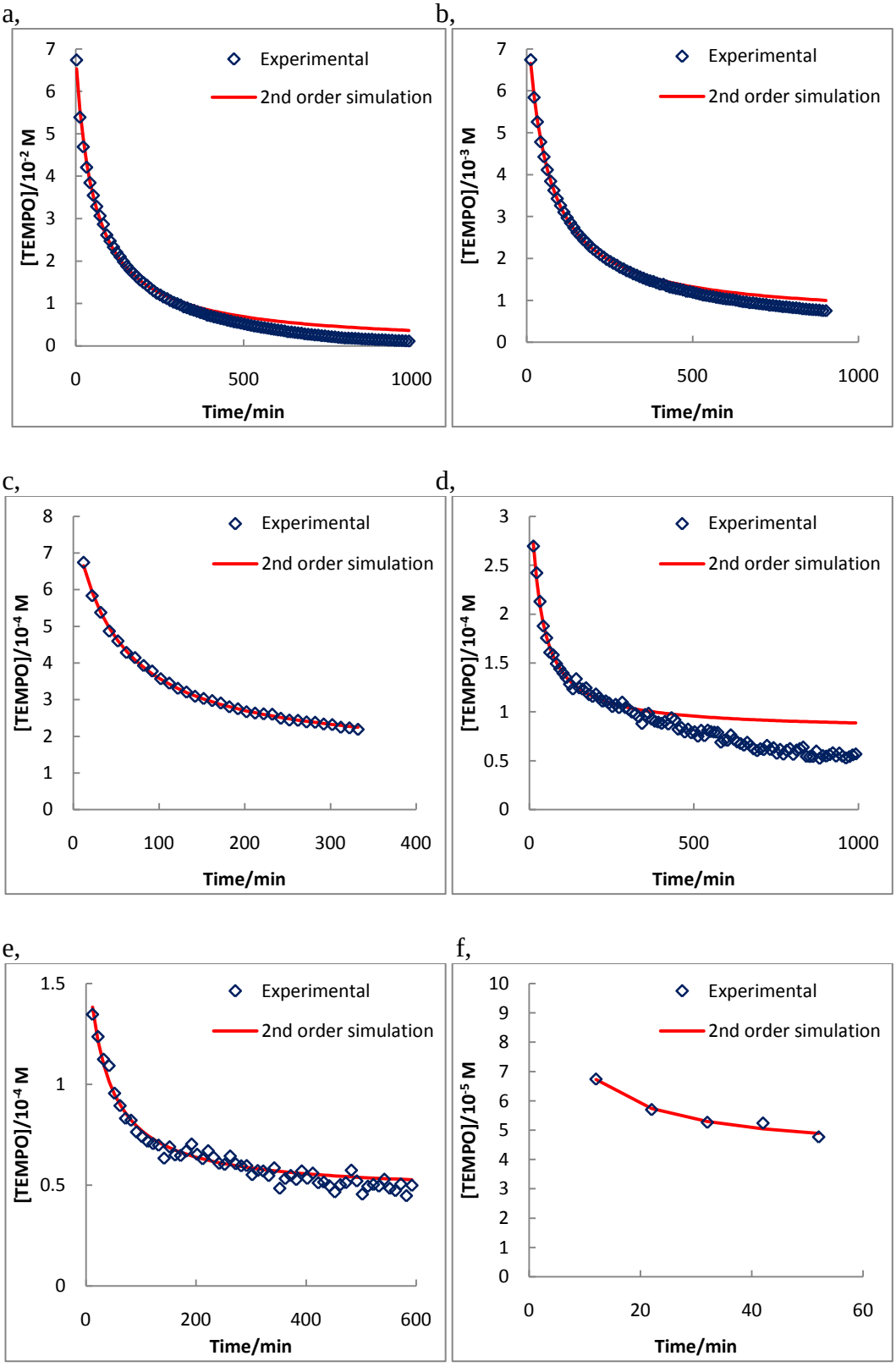

Figure 3. 20. Kinetic profiles and 2nd-order fitting of TEMPO decay in acrylic acid at 100 ℃. TEMPO concentration: a, 1%. b, 0.1%. c, 100ppm. d, 40ppm. e, 20ppm. f, 10ppm.

All kinetic data were then normalized in order to fit to a simple kinetic model. However, this has not been successful because rate constant acquired from each concentration varied significantly (Table 3.6).

Table 3. 6. Rate constants obtained from TEMPO decay in acrylic acid at 100 ℃ starting from various initial concentrations.

C_0(mass ratio)	C_0(mol/L)	k($M^{-1}\cdot s^{-1}$)
1%	6.71×10^{-2}	3.74×10^{-2}
1000ppm	6.71×10^{-3}	2.07×10^{-3}
100ppm	6.71×10^{-4}	1.18×10^{-3}
40ppm	2.68×10^{-4}	2.36×10^{-4}
20ppm	1.34×10^{-4}	1.82×10^{-5}
10ppm	6.71×10^{-5}	1.71×10^{-6}

The deviation of reaction kinetic profile from 2^{nd}-order and inconsistent rate constants suggest complexity of this reaction.

3.4.2.3. Nitroxide radical disproportionation in acetic and propionic acid

In order to clarify if the complexity of the reaction is due to radical processes which involves the vinyl group of acrylic acid, 4HT decay and oxygen consumption in saturated organic acids were studied for comparison. Unexpectedly, oxygen depletion was also observed since the linewidth of 4HT EPR spectra were sharpened over time. The 4HT intensity decay and oxygen consumption are shown in Figure 3.21.

a, b,

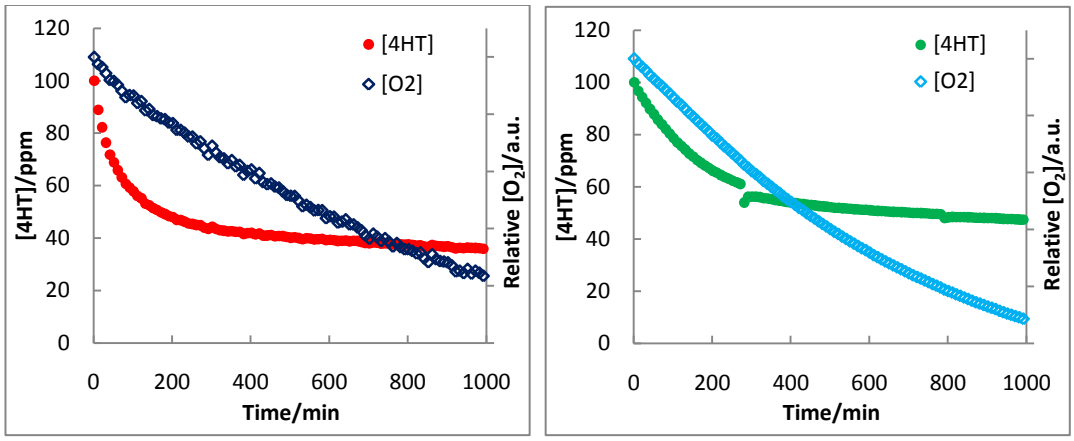

Figure 3. 21. 4HT (●) and oxygen (◊) decay of an acetic acid solution of 100ppm 4HT at 100 ℃. b, 4HT (●) and oxygen (◊) decay of a propionic acid solution of 100ppm 4HT at 100 ℃.

Oxygen consumption in acrylic acid was assumed to be related to generation of alkyl radicals in the autoxidation process under heating. In saturated organic acid, oxygen depletion could be due to oxidation of 4HT or autoxidation of the solvent (Scheme 3.26, p93). Incomplete ionization of organic acids also complicates the system. For further simplification, this reaction needs to be studied in mineral acid instead of organic acids, because the reaction in mineral acid can be an excellent model system for organic acidic monomers.

3.4.2.4. TEMPO disproportionation in sulphuric acid

In order to establish a model system for organic acidic monomers, TEMPO disproportionation reaction was studied in a mineral acid. Among common mineral acids, nitric acid can act as an oxidizing agent which would complicate the investigation. Hence, nitric acid was ruled out. Hydrochloric acid is volatile. As a result, concentration of hydrochloric acid solution would vary over time, especially at high temperature. Therefore, hydrochloric acid was also ruled out. Sulphuric acid was chosen for this study because of its non-oxidizing nature and its stability of concentration under different conditions.

In sulphuric acid, three different types of TEMPO EPR spectra can be obtained at different concentrations of acid (Figure 3.22). In dilute acid solution (*e.g.* 0.1M H_2SO_4), TEMPO is the main component in the reaction mixture with only a small amount of protonated TEMPO. TEMPO gives a triplet EPR spectrum due to the hyperfine coupling interaction between the free electron and the nitrogen atom. In more concentrated solution (*e.g.* 50%-80% H_2SO_4), the fast proton transfer between TEMPO and protonated TEMPO is on the EPR times scale (*ca.* 10^{-9}s)[78], which leads to broadening of the EPR spectra beyond detection. In concentrated sulphuric acid (*e.g.* 98% H_2SO_4), TEMPO can be fully protonated. The EPR spectrum of protonated TEMPO is a triplet of doublets, because the free electron is coupling with both the hydrogen and nitrogen atoms.

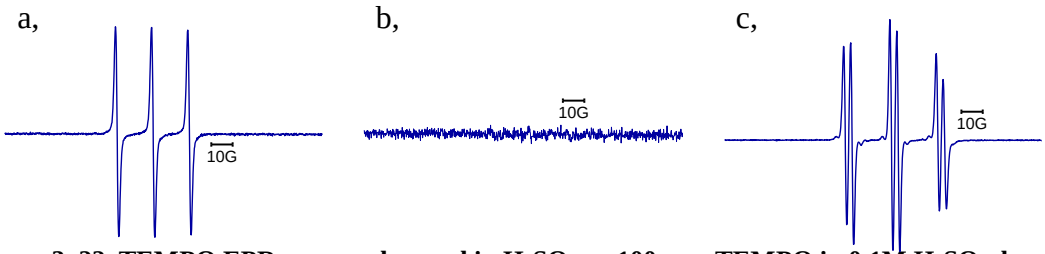

Figure 3. 22. TEMPO EPR spectra detected in H_2SO_4. a, 100ppm TEMPO in 0.1M H_2SO_4. b, 100ppm TEMPO in 80% H_2SO_4. c, 100ppm TEMPO in 98% H_2SO_4.

EPR spectrum of protonated TEMPO has been previously reported by Hoffman *et al.*[79], who protonated TEMPO with Lewis acids (*e.g.* $AlCl_3$). Fully protonated TEMPO is stable, as its EPR signal lasts for days without significant disproportionation. Fast disproportionation is only observed for partially protonated TEMPO. Therefore the disproportionation must be a reaction between TEMPO and its protonated form, which yields the corresponding TEMPOH and oxoammonium cation (Scheme 3.45).

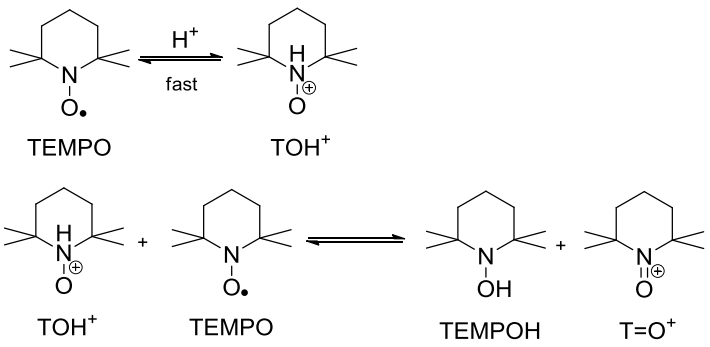

Scheme 3. 45. Protonation of TEMPO followed by reaction between TEMPO and its protonated form to yield TEMPOH and *N*-oxoammonium cation.

Both UV and EPR were used to monitor TEMPO disproportionation in H_2SO_4. TEMPO and oxoammonium chloride salt have distinctive UV absorbance at 425nm and 465nm, respectively. The two molecules are thus distinguishable by UV. The clear red-shift upon the reaction of TEMPO with sulphuric acid indicates consumption of TEMPO and formation of oxoammonium salt (Figure 3.23).

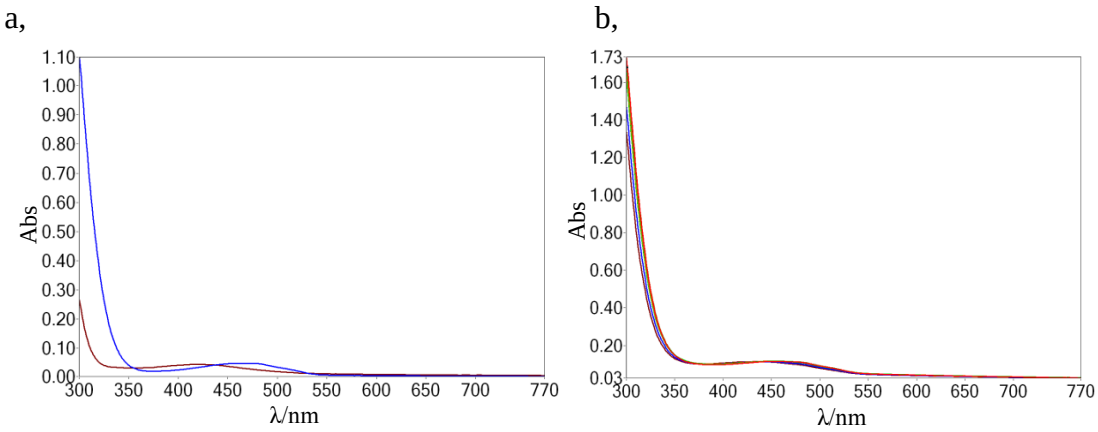

Figure 3. 23. a, UV spectra of 2×10^{-6}M TEMPO (in brown) and 2×10^{-6}M $T=O^+$ (in blue) in H_2O. b, 2×10^{-6}M TEMPO in 1M H_2SO_4 at R.T. at different reaction times. Red shift of the absorbance was observed.

EPR study was carried out to acquire accurate kinetic data of TEMPO decay. This was achieved by measuring the intensity of TEMPO EPR signal. The reaction of TEMPO decay in H_2SO_4 (aq) at room temperature (*e.g.* 6.41×10^{-4} M TEMPO in an aqueous solution of 0.1 M H_2SO_4) showed good fit to a 2nd-order kinetic model. The kinetic profile and fitting is shown in Figure 3.24.

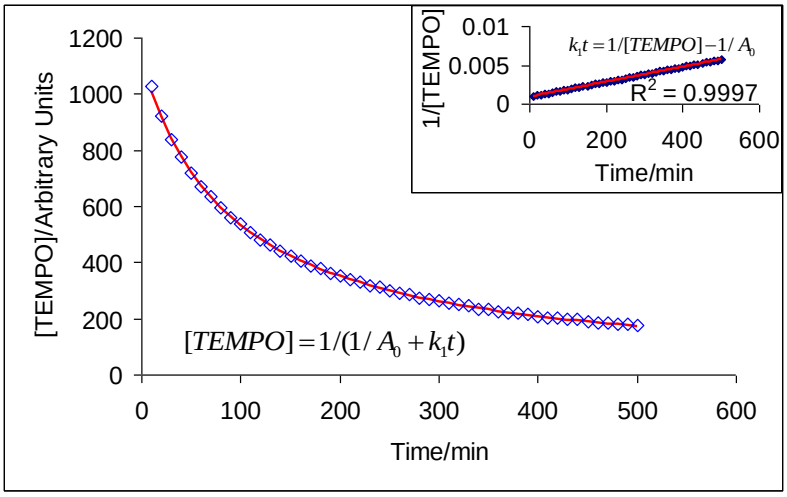

Figure 3. 24. 100ppm TEMPO decay in 0.1 M H_2SO_4 at R.T. monitored by EPR. Inset: Plot of 1/[TEMPO] versus time.

TEMPO disproportionation was also monitored at various concentration of H_2SO_4 at room temperature and at high temperature (*e.g.* 80 ℃) which is closer to the real application conditions. However, the fitting at high temperature was not satisfactory. It was also noticed that the initial intensity of TEMPO varies according to different concentration of H_2SO_4 (Figure 3.25). This effect is more evident at high temperature.

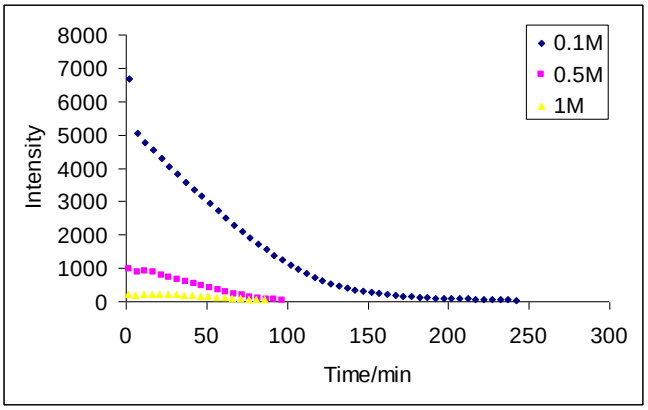

Figure 3. 25. Decay of 2000ppm TEMPO in different concentration of H_2SO_4 at 80 ℃ monitored by EPR.

The observation of such effect indicates that the disproportionation reaction is very fast in strong acid. The reaction is almost finished before it is monitored. Unfortunately it is difficult to study such a fast reaction at high temperature using normal techniques. The most common technique for studying fast reactions by EPR

spectroscopy is stopped-flow. However, stopped-flow experiment at high temperature is complicated. Therefore, a temperature dependent kinetic model was built at lower temperature to predict TEMPO disproportionation at high temperature.

3.4.3. Temperature dependent kinetic model of TEMPO disproportionation

3.4.3.1. Kinetic model of TEMPO disproportionation reaction

Due to the difficulties of studying the disproportionation reaction at high temperature directly, it was feasible to obtain temperature dependent rate constants from low temperature experiments and extrapolate them to high temperature. TEMPO disproportionation in inorganic acids at low temperature (*e.g.* below 50 ℃) has been studied by Golubev *et al.* in the 1970s[80] and revised recently[11]. Adequate kinetic data were generated in their study, however, a kinetic model of this reaction was not built. Thus, by using the reported kinetic constants, a full kinetic model was built to predict TEMPO disproportionation reaction using the following procedure:-

The reaction was assumed to involve four steps.

1. Protonation of TEMPO: fast equilibrium
2. Relatively slow disproportionation
3. Comproportionation of TEMPOH and oxoammonium salt
4. Protonation of TEMPOH.

Hence the reaction is described by the following equations.

$T + H^+ \rightleftharpoons TH^+$ Ka_1

$(T + H^+ \underset{k_{-1}}{\overset{k_1}{\rightleftharpoons}} TH^+)$

$T + TH^+ \longrightarrow TOH + T{=}O^+$ k_2

$TOH + T{=}O^+ \longrightarrow T + TH^+$ k_{-2}

$TOH + H^+ \rightleftharpoons TOH_2^+$ Ka_3

Here, Ka_1 and Ka_3 are acid dissociation constants of TEMPO (T) and TEMPOH (TOH), respectively. TH^+, $T{=}O^+$, TOH_2^+ represents protonated TEMPO, *N*-oxoammonium cation and protonated TEMPOH, respectively.

In order to build a kinetic model it was assumed that under the reaction conditions, the amount of protonated TEMPO and unprotonated TEMPOH in the reaction mixture is negligible. Thus the concentration equations of reagents can be written as:

$$d[T]/dt = -2k_2 [T]_t [TH^+]_t + k_{-2}[TOH]_t[T{=}O^+]_t$$

$$[TH^+]_t=[T]_t[H^+]/Ka_1$$

$$d[T{=}O^+]/dt=k_2[T]_t[TH^+]_t - k_{-2}[TOH]_t[T{=}O^+]_t$$

$$d[TOH_2^+]/ dt=k_2[T]_t[TH^+]_t - k_{-2}[TOH]_t[T{=}O^+]_t$$

$$[TOH]= [T]_tKa_3/[H^+]$$

Temperature dependence of k_{-2} and k_2/k_{-1} was reported in Golubev's study[80]:

$$\lg k_2/Ka_1=13.70-19500/4.575T$$

$$\lg k_{-2}=17.77-21900/4.575T$$

Here, the units for rate constants, dissociation constant temperature (T) are $M^{-1}{\cdot}s^{-1}$, M and K respectively.

Therefore the concentration equations are modified to the following equations:

$$d[T]/dt = -2k_2 [T]_t^{\,2}[H^+] + k_{-2}[TOH]_t[T{=}O^+]_t$$

$$[TH^+]_t=[T]_t[H^+]/Ka_1$$

$$d[T{=}O^+]/dt=k_2[T]_t^{\,2}[H^+] - k_{-2}[TOH]_t[T{=}O^+]_t$$

$$d[TOH_2^{\,+}]/\,dt= k_2[T]_t^{\,2}[H^+] - k_{-2}[TOH]_t[T{=}O^+]_t$$

$$[TOH]= [T]_tKa_3/[H^+]$$

A user-friendly kinetic model of TEMPO disproportionation was thus built by applying the equations in an Excel spreadsheet. Reaction parameters including initial concentrations of TEMPO and acid, reaction temperature and reaction time scale can be modified by the user. TEMPO decay and oxoammonium cation/TEMPOH formation are plotted. One can adjust the reaction parameters to predict the reaction rate at the desired conditions. The simulated kinetic curves at some typical conditions are shown in Figure 3.26.

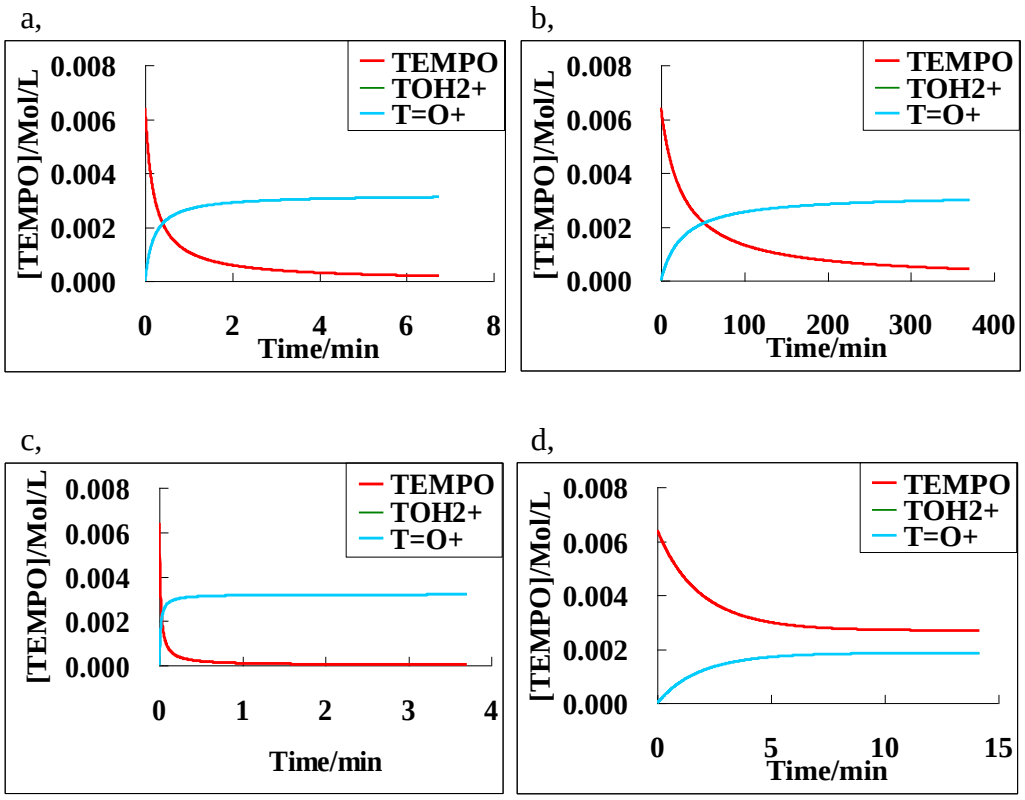

Figure 3. 26. Simulated TEMPO, oxoammonium salt and protonated hydroxylamine evolution in acid under different reaction conditions: a, 6.4×10^{-3}M TEMPO in 0.1M H_2SO_4 at 25 ℃. b,

6.4×10^{-3}M TEMPO in 1M H_2SO_4 at 25 ℃.. c, 6.4×10^{-3}M TEMPO in 1M H_2SO_4 at 80 ℃. d, 6.4×10^{-3}M TEMPO in 0.005M H_2SO_4 at 80 ℃

It is clear that the reaction in 0.1M H_2SO_4 at room temperature is a slow disproportionation which takes as long as 400 minutes. In 1M H_2SO_4 at room temperature, this reaction is much faster with disproportionation almost complete in less than 10 minutes. In 0.005M H_2SO_4 the prediction clearly shows this reaction reaches equilibrium and TEMPO concentration remains constant. In 1M H_2SO_4 at 80 ℃ the disproportionation is very fast, as equilibrium is reached within 1 minute.

3.4.3.2. Fitting experimental data to the kinetic model

At low temperature

At room temperature, our experimental data fits the kinetic model precisely (Figure 3.27). Little adjustment needs to be made and the fitting quality is satisfactory.

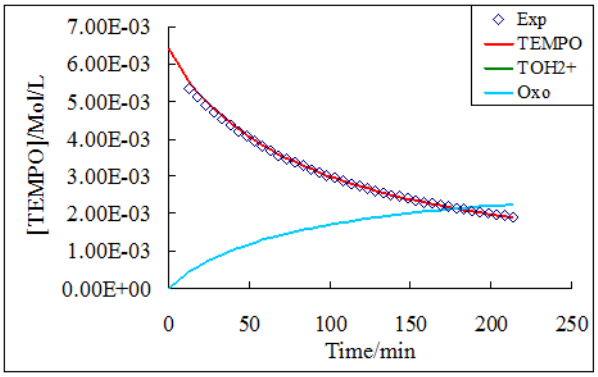

Figure 3. 27. Fitting experimental kinetic data of 1000ppm TEMPO in 0.1M H_2SO_4 at 15 ℃ to kinetic model.

At high temperature

At high temperature, TEMPO decay seems to be much more complicated. Significant deviation was observed while fitting experimental kinetic data to the model (Figure 3.28).

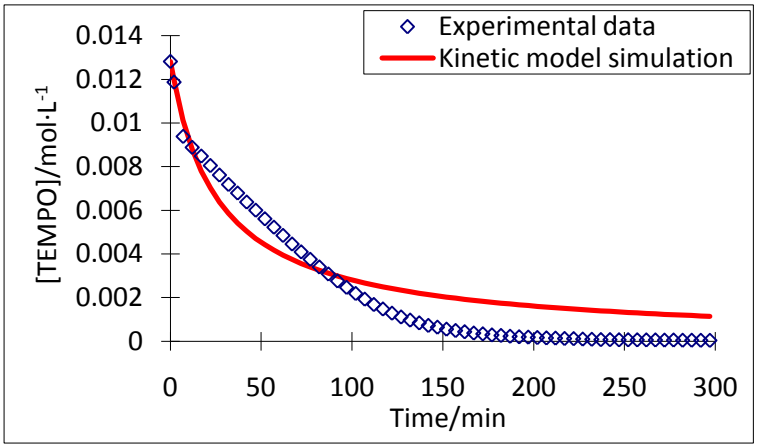

Figure 3. 28. Fitting experimental kinetic data of 1.28×10^{-2} M TEMPO in 0.1M H_2SO_4 at 80 ℃ to the kinetic model.

This suggests that the reaction at high temperature is more complicated. Some side reactions that were negligible at low temperature become significant at high temperature.

3.4.4. Comproportionation of TEMPOH and *N*-oxoammonium salt

The disproportionation reaction of TEMPO gives rise to the corresponding oxoammonium cation and TEMPOH, which are the two key molecules in the catalytical activities of TEMPO. Oxoammonium salt is a strong oxidizing agent. TEMPOH can be oxidized by oxoammonium salt in neutral pH and comproportionate to form nitroxide. However, TEMPOH can be protonated in acid which stabilizes it. This makes the comproportionation reaction pH-dependent. To determine if disproportionation is fully reversible, a stopped-flow experiment was carried out. Immediately following mixing of 2×10^{-3} M TEMPOH and 2×10^{-3} M oxoammonium salt at different pH with the stopped-flow equipment, a time scan was applied on the magnetic field corresponding to the first EPR peak of TEMPO signal. Kinetic profiles of the comproportionation reaction at different pH were thus obtained (Figure 3.29).

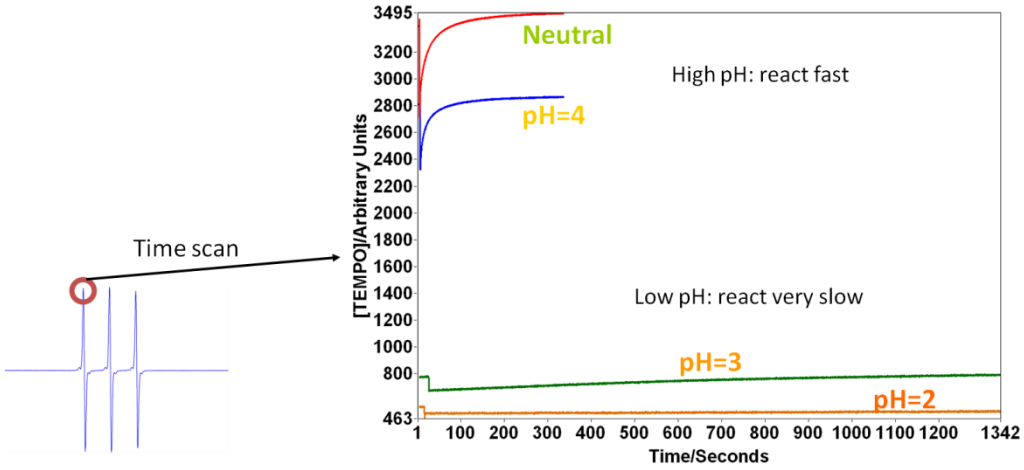

Figure 3. 29. TEMPO formation vs. time in comproportionation reaction of 2×10^{-3} M TEMPOH and 2×10^{-3} M oxoammonium salt at different pH.

It is clear that comproportionation is slow at low pH but very fast at neutral pH. This result is consistent with previously reported data by Goldstein and co-workers[81]. It is also noticed that the position of equilibrium changed according to different acidity. The disproportionation of TEMPO takes place in acid because hydroxylamine is protected by protonation. However the reverse reaction in the absence of acid is thermodynamically preferable. Therefore, disproportionation reaction is reversible.

Neutralization of such reaction mixture can result in recovery of decayed TEMPO intensity back instantly. As shown in the Figure 3.30, TEMPO decay at room temperature is fully reversible upon neutralization with $NaHCO_3$ to the original intensity regardless of the reaction time. This result indicates that at room temperature no side reaction takes place.

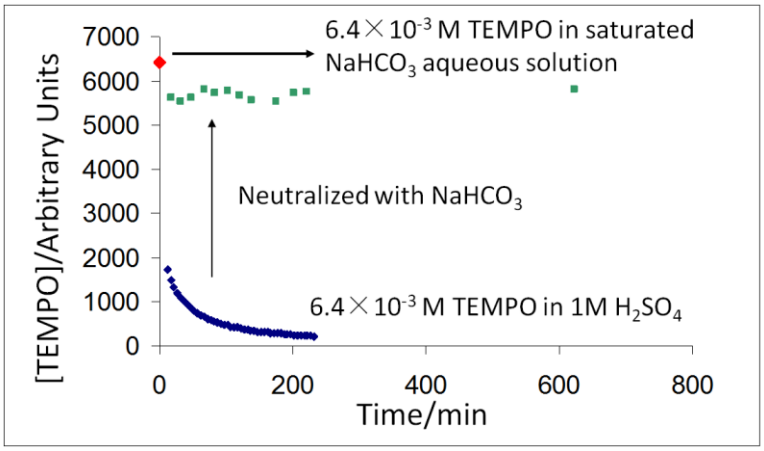

Figure 3. 30. a, EPR signal decay of 6.4×10^{-3} M TEMPO in 1M H_2SO_4 at R.T. (in blue). b, EPR signal intensity of 6.4×10^{-3} M TEMPO in 1M H_2SO_4 at R.T. after neutralization with excess $NaHCO_3$, at different reaction times (in green). c, 6.4×10^{-3} M TEMPO in saturated $NaHCO_3$ solution (in red).

3.4.5. Conclusions of acid-catalyzed TEMPO disproportionation

Acid catalyzed disproportionation of TEMPO and derivatives was studied using EPR and UV spectroscopy. The reaction in mineral acid at room temperature is well-understood (Scheme 3.46). TEMPO can be protonated in acid. Protonated TEMPO alone is stable, however, it can react with neutral TEMPO and disproportionate to form the corresponding hydroxylamine and oxoammonium salt. Hydroxylamine is also protonated which prevents re-oxidation by oxoammonium salt. Comproportionation reaction of hydroxylamine and oxoammonium salt is pH-dependent. It is fast at neutral pH but slow at low pH. Neutralization of reaction mixture thus results in the recovery of TEMPO EPR signal. At room temperature, there are no further reactions except the protonation and disproportionation. A kinetic model was built according to literature temperature-dependent rate constants. Fitting room temperature kinetic data to this model is satisfactory.

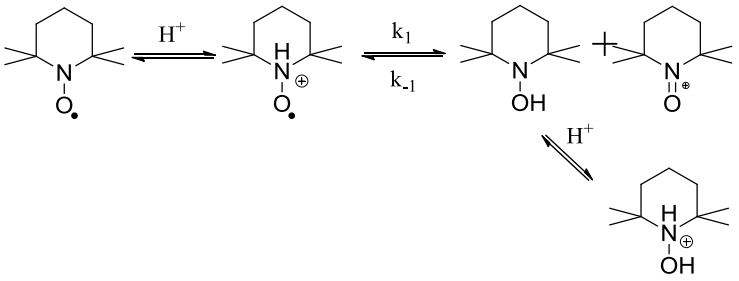

Scheme 3. 46. TEMPO disproportionation in acid.

3.5. Conclusions

In this chapter, a novel method to investigate the mechanism of nitroxide-based antioxidant is demonstrated. EPR oximetry via convolution-based fitting method provides one with unique advantages for studying such systems. It permits simultaneous determination of both nitroxide and oxygen consumption. Application of this method to neutral target monomers such as styrene, methyl methacrylate and acrylonitrile lead to better understanding of the system. Formation of peroxyl radicals from oxygen and the propagation radicals is the primary inhibition mechanism in the beginning of self-initiated polymerization. When oxygen depletes, nitroxides quench alkyl radicals. Different self-initiation rate also suggest Mayo mechanism is the major route in the self-initiation process in styrene. In monomers such as methyl methacrylate and acrylonitrile, Diels-Alder reaction is not possible. Therefore a lack of efficient self-initiation mechanism makes oxygen consumption significantly slower than in styrene.

In acidic monomer, acrylic acid, this fitting method was also adopted to the investigation on the polymerization inhibition mechanism of nitroxides and the synergistic effect with other inhibitors. The synergism of nitroxide with phenol-type inhibitors (*e.g.* MEHQ) depends on the reversible hydrogen abstraction between nitroxide and the phenol. Hydroxylamine was found to play an important role in the synergistic inhibition mechanism of nitroxide and PTZ mixture. In the presence of acid, hydroxylamine is a significant component in the mixture of nitroxide and PTZ.

Quenching of alkyl and peroxyl radicals by hydroxylamine is thus a major inhibition mechanism.

The fast decay of nitroxide inhibitors in acidic monomers (*e.g.* acrylic acid) is due to the acid catalyzed disproportionation reaction. This reaction was studied thoroughly using a model system of TEMPO in sulphuric acid. The result shows TEMPO can be protonated in acid, leading to formation of the corresponding TEMPO precursor hydroxylamine and *N*-oxoammonium cation. In acidic conditions, hydroxylamine is also protonated which minimizes comproportionation. Comproportionation of hydroxylamine and oxoammonium salt is fast at neutral pH but slow at low pH. A kinetic model was built using literature data to predict disproportionation reaction. Our experimental data were fitted to the kinetic model. At room temperature, the fitting is perfect. However, at high temperature, a deviation is often found. In fact, the kinetic profile of nitroxide in acid at high temperature is not compatible with a simple kinetic model. Hence, next chapter details the study of TEMPO decay at high temperature.

References:

1. H. Hayat and B. L. Silver, *The Journal of Physical Chemistry*, 1973, **77**, 72-78.
2. H.-C. Shi and Y. Li, *J. Mol. Catal. A: Chem.*, 2007, **271**, 32-41.
3. L. B. Volodarsky, V. A. Reznikov and V. I. Ovcharenko, *Synthetic Chemistry of Stable Nitroxides*, CRC Press, Boca Raton, 1994.
4. O. L. Lebedev and S. N. Kazarnovskii, *Zh. Obshch. Khim.*, 1960, **30**, 1631-1635.
5. J. L. Hodgson, M. Namazian, S. E. Bottle and M. L. Coote, *J. Phys. Chem. A*, 2007, **111**, 13595-13605.
6. V. A. Golubev, E. G. Rozantsev and M. B. Neiman, *Russ. Chem. Bull.*, 1965, 1898-1904.
7. L. O. Atovmyan, V. A. Golubev, N. I. Golovina and G. A. Klitskaya, *J. Struct. Chem.*, 1975, **16**, 79-83.
8. V. Golubev, V. Borislavskii and A. Aleksandrov, *Russ. Chem. Bull.*, 1977, **26**, 1874-1881.
9. A. Samuni, S. Goldstein, A. Russo, J. B. Mitchell, M. C. Krishna and P. Neta, *J. Am. Chem. Soc.*, 2002, **124**, 8719-8724.
10. A. Nilsen and R. Braslau, *J. Polym. Sci., Part A: Polym. Chem.*, 2006, **44**, 697-717.
11. V. D. Sen and V. a. Golubev, *J. Phys. Org. Chem.*, 2009, **22**, 138-143.
12. M. Lucarini and G. F. Pedulli, *Chem. Soc. Rev.*, 2010, **39**, 2106-2106.
13. J. J. Warren and J. M. Mayer, *J. Am. Chem. Soc.*, 2008, **130**, 2774-2776.
14. M. Lucarini, F. Ferroni, G. F. Pedulli, S. Gardi, D. Lazzari, G. Schlingloff and M. Sala, *Tetrahedron Lett.*, 2007, **48**, 5331-5334.
15. M. I. de Heer, H.-G. Korth and P. Mulder, *J. Org. Chem.*, 1999, **64**, 6969-6975.
16. X.-M. Zhang, *J. Org. Chem.*, 1998, **63**, 1872-1877.
17. J. M. Simmie, G. Black, H. J. Curran and J. P. Hinde, *J. Phys. Chem. A*, 2008, **112**, 5010-5016.
18. I. O. Opeida, A. G. Matvienko, O. Z. Bakurova and R. A. Voloshkin, *Russ. Chem. Bull.*, 2003, **52**, 900-904.
19. J. M. Mayer and I. J. Rhile, *BBA-Bioenergetics*, 2004, **1655**, 51-58.

20. F. G. Bordwell and W.-Z. Liu, *J. Am. Chem. Soc.*, 1996, **118**, 10819-10823.
21. G. Moad and D. H. Solomon, *The Chemistry of Radical Polymerization*, 2nd Edition edn., Elsevier, Oxford, 2006.
22. M. V. Ciriano, H. G. Korth and W. B. V. Scheppingen, *J. Am. Chem. Soc.*, 1999, **121**, 6375-6381.
23. W. G. Skene, S. T. Belt, T. J. Connolly, P. Hahn and J. C. Scaiano, *Macromolecules*, 1998, **31**, 9103-9105.
24. J. Trnka, F. H. Blaikie, R. a. J. Smith and M. P. Murphy, *Free Radical Biol. Med.*, 2008, **44**, 1406-1419.
25. G. Moad, E. Rizzardo and S. H. Thang, *Acc. Chem. Res.*, 2008, **41**, 1133-1142.
26. A. A. Gridnev, *Macromolecules*, 1997, **30**, 7651-7654.
27. W. Braunecker and K. Matyjaszewski, *Prog. Polym. Sci.*, 2007, **32**, 93-146.
28. K. Platkowski and K. H. Reichert, *Chem. Eng. Technol.*, 1999, **22**, 1035-1038.
29. G. I. Likhtenshtein, J. Yamauchi, S. i. Nakatsuji, A. I. Smirnov and R. Tamura, *Nitroxides: Applications in Chemistry, Biomedicine, and Materials Science*, WILEY-VCH verlag GmbH & Co. KGaA, Weinheim, 2008.
30. E. E. Voest, E. Vanfaassen and J. J. M. Marx, *Free Radical Biol. Med.*, 1993, **15**, 589-595.
31. S. Suy, J. B. Mitchell, D. Ehleiter, A. Haimovitz-Friedman and U. Kasid, *J. Biol. Chem.*, 1998, **273**, 17871-17878.
32. S. I. Dikalov, A. E. Dikalova and R. P. Mason, *Arch. Biochem. Biophys.*, 2002, **402**, 218-226.
33. A. Dijksman, A. Marino-Gonzalez, A. M. I. Payeras, I. Arends and R. A. Sheldon, *J. Am. Chem. Soc.*, 2001, **123**, 6826-6833.
34. T. Fey, H. Fischer, S. Bachmann, K. Albert and C. Bolm, *J. Org. Chem.*, 2001, **66**, 8154-8159.
35. X. Wang, R. Liu, Y. Jin and X. Liang, *Chemistry (Weinheim an der Bergstrasse, Germany)*, 2008, **14**, 2679-2685.
36. R. A. Sheldon and I. Arends, *Adv. Synth. Catal.*, 2004, **346**, 1051-1071.
37. A. E. J. Denooy, A. C. Besemer and H. Vanbekkum, *Tetrahedron*, 1995, **51**, 8023-8032.

38. N. Merbouh, J. M. Bobbitt and C. Bruckner, *Tetrahedron Lett.*, 2001, **42**, 8793-8796.
39. N. Merbouh, J. M. Bobbitt and C. Bruckner, *J. Org. Chem.*, 2004, **69**, 5116-5119.
40. F. R. Mayo, *J. Am. Chem. Soc.*, 1968, **90**, 1289-1295.
41. F. R. Mayo, *J. Am. Chem. Soc.*, 1953, **75**, 6133-6141.
42. H. K. H. Jr., *Angew. Chem. Int. Ed.*, 1983, **22**, 440-455.
43. H. K. Hall and A. B. Padias, *Acc. Chem. Res.*, 1990, **23**, 3-9.
44. K. U. Ingold, *Chem. Rev.*, 1961, **61**, 563-589.
45. E. T. Denisov, *Dokl. Akad. Nauk. SSSR*, 1960, **130**, 1055-1058.
46. E. T. Denisov and I. B. Afanas'ev, *Oxidatoin and Antioxidants in Organic Chemistry and Biology*, Taylor & Francis, Amsterdam, 2005.
47. E. T. Denisov, *Handbook of Antioxidants: Bond Dissociation Energies, Rate Constants, Activation Energies and Enthalpies of Reactions*, CRC Press, Boca Raton, 1995.
48. L. B. Levy, *J. Polym. Sci., Part A: Polym. Chem.*, 1985, **23**, 1505-1515.
49. L. B. Levy, *J. Appl. Polym. Sci.*, 1996, **60**, 2481-2487.
50. S. Schulze and H. Vogel, *Chem. Eng. Technol.*, 1998, **21**, 829-837.
51. M. F. Chiu, B. C. Gilbert and P. Hanson, *Journal of the Chemical Society B: Physical Organic*, 1970, 1700-1708.
52. F. L. Rupérez, J. C. Conesa and J. Soria, *Spectrochim. Acta, Pt. A: Mol. Spectrosc.*, 1984, **40**, 1021-1024.
53. A. A. Ivanov, G. M. Lysenko, A. I. Kadantseva and In, *Polym. Sci. USSR*, 1981, 689-695.
54. L. B. Levy, *J. Polym. Sci., Part A: Polym. Chem.*, 1992, **30**, 569-576.
55. Y. B. Shilov, Battalov.Rm and E. T. Denisov, *Dokl. Akad. Nauk. SSSR*, 1972, **207**, 388-&.
56. R. Amorati, G. F. Pedulli, D. a. Pratt and L. Valgimigli, *Chem. Commun.*, 2010, **2010**, 5139-5141.
57. J. M. Vanderkooi, M. Erecinska and I. A. Silver, *Am. J. Physiol.*, 1991, **260**, C1131-C1150.
58. L. C. Clark, *T. Am. Soc. Art. Int. Org.*, 1956, **2**, 41-48.
59. W. J. Whalen, J. Riley and P. Nair, *J. Appl. Physiol.*, 1967, **23**, 798-801.

60. M. E. Towell, I. Lysak, E. C. Layne and S. P. Bessman, *J. Appl. Physiol.*, 1976, **41**, 245-250.
61. J. R. Lakowicz and G. Weber, *Biochemistry*, 1973, **12**, 4161-4170.
62. W. R. Ware, *J. Phys. Chem.*, 1962, **66**, 455-458.
63. J. A. O'Hara, H. G. Hou, E. Demidenko, R. J. Springett, N. Khan and H. M. Swartz, *Physiol. Meas.*, 2005, **26**, 203-213.
64. R. Ahmad and P. Kuppusamy, *Chem. Rev.*, 2010, **110**, 3212-3236.
65. B. Gallez, B. F. Jordan, C. Baudelet and P. D. Misson, *Magn. Reson. Med.*, 1999, **42**, 627-630.
66. G. Ilangovan, T. Liebgott, V. K. Kutala, S. Petryakov, J. L. Zweier and P. Kuppusamy, *Magn. Reson. Med.*, 2004, **51**, 835-842.
67. J. F. Dunn, J. A. O'Hara, Y. Zaim-Wadghiri, H. Lei, M. E. Meyerand, O. Y. Grinberg, H. G. Hou, P. J. Hoopes, E. Demidenko and H. M. Swartz, *J. Magn. Reson. Im.*, 2002, **16**, 511-521.
68. M. Conte, Y. Ma, C. Loyns, P. Price, D. Rippon and V. Chechik, *Org. Biomol. Chem.*, 2009, **7**, 2685-2687.
69. B. Gallez, R. Debuyst, F. Dejehet, K. J. Liu, T. Walczak, F. Goda, R. Demeure, H. Taper and H. M. Swartz, *Magn. Reson. Med.*, 1998, **40**, 152-159.
70. N. Vahidi, R. B. Clarkson, K. J. Liu, S. W. Norby, M. Wu and H. M. Swartz, *Magn. Reson. Med.*, 1994, **31**, 139-146.
71. B. Gallez, R. Debuyst, K. J. Liu, R. Demeure, F. Dejehet and H. M. Swartz, *Magn. Reson. Mater. Phy.*, 1996, **4**, 71-75.
72. N. M. Atherton, *Principles of Electron Spin Resonance*, Ellis Horwood; PTR Prentice Hall, New York, 1993.
73. G. F. Pedulli, M. Lucarini, P. Pedrielli, M. Sagrini and M. Cipollone, *Res. Chem. Intermed.*, 1996, **22**, 1-14.
74. T. I. Smirnova and A. I. Smirnov, in *ESR Spectroscopy in Membrane Biophysics*, eds. M. A. Hemminger and L. J. Berliner, Springer, Amsterdam, Editon edn., 2007.
75. A. Trubnikov, M. Goldfein, N. Kozhevnikov, E. Rafikov, A. Stepukhovich and V. Tomashchuk, *Polym. Sci. USSR*, 1978, **20**, 2751-2758.
76. G. Landi, L. Lisi and G. Russo, *J. Mol. Catal. A: Chem.*, 2005, **239**, 172-179.

77. H. M. Zhang, X. Q. Ruan, Q. X. Guo and Y. C. Liu, *Res. Chem. Intermed.*, 1998, **24**, 687-693.

78. A. Schweiger and G. Jeschke, *Principles of Pulse Electron Paramagnetic Resonance*, Oxford University Press, Oxford, 2001.

79. B. M. Hoffman and T. B. Eames, *J. Am. Chem. Soc.*, 1969, **91**, 2169-2170.

80. V. A. Golubev, V. D. Sen, I. V. Kulyk and A. L. Aleksandrov, *B. Acad. Sci. USSR Ch.*, 1975, **24**, 2119-2126.

81. A. Israeli, M. Patt, M. Oron, A. Samuni, R. Kohen and S. Goldstein, *Free Radical Biol. Med.*, 2005, **38**, 317-324.